# SENSOR APPLICATIONS OF POLYMER FIELD EFFECT TRANSISTORS

by
İsmail Terkeşli
B.S., Electrical and Electronics Engineering, Boğaziçi University, 2010

Submitted to the Institute for Graduate Studies in
Science and Engineering in partial fulfillment of
the requirements for the degree of
Master of Science

Graduate Program in Electrical and Electronics Engineering Department
Boğaziçi University
2013

# ACKNOWLEDGEMENTS

I would like to express the deepest appreciation to my thesis supervisor Assoc. Prof. Şenol Mutlu for his encouragements, comments and suggestions. Without his guidance and excitement in researching and teaching, this thesis would not have been possible.

I also would like to specially thank my project friend Berkan Yaman for his help, motivation and friendship both at work and after work. I also thank to Orhan Mert and Merve Türksoy for their valuable helps. My thanks are extended to Abdullah Sarıduman, Barış Esen, Gökhan Hacıahmetoğlu, İsmail Kara and Kenan Türksoy for their friendships, funny talks and leisure activities.

I am very grateful to love of my life Müge Kirman for everything we share together.

Finally, I am most grateful to my dear parents Müzeyyen and Ali Terkeşli with my sisters, Dilara and Esra, for their lifelong love and supports under all circumstances.

This study is supported by Turkish Scientific and Technological Research Council (TUBITAK) project 110E063.

# ABSTRACT

## SENSOR APPLICATIONS OF POLYMER FIELD EFFECT TRANSISTORS

This thesis presents the fabrication and characterization of organic field effect transistors (OFETs) for sensor applications using polymeric semiconductor of poly (3-hexyl thiophene)(P3HT). Utilizing deionized (DI) water as gate insulator, operation voltages of polymer field effect transistors (polymer FETs) are reduced below 1V. To ease the microfluidic channel integration of polymer FETs, a novel structure called planar OFET is designed and introduced. Comparing the output characteristics of planar OFET with the one of top-gate, bottom-contact OFET using gate probe in stead of deposited gate electrode, it is shown that this planar OFET topology operates successfully as field effect transistor providing on-off ratio of about 50. It is stated that P3HT film deposition by spin-coating method leads higher on-off ratios than drop-casting method for top-gate, bottom-contact OFET topology. Then, durability of P3HT to microfabrication processes is examined. In addition, sensitivity of P3HT to NaCl and KCl solutions is searched. Finally, microfluidic channel encapsulation of planar polymer FETs with three different materials, polyvinyl alcohol (PVA), parylene and polydimethylsiloxane (PDMS) is searched. PVA microfluidic channels providing liquid flow are successfully formed. On-off ratios of 4 and 10 are obtained with planar polymer FETs integrated into parylene and PDMS microfluidic channels, respectively.

# ÖZET

## POLİMER ALAN ETKİLİ TRANSİSTÖRLERİN SENSÖR UYGULAMALARI

Bu tez polimer yarıiletken olarak poli (3-hekzil tiyofen)(P3HT) kullanan organik alan etkili transistörlerin (OFET) sensör uygulamaları için fabrikasyon ve karakterizasyonunu sunmaktadır. Kapı yalıtkanı olarak deiyonize (DI) sudan yararlanılarak, polimer alan etkili transistörlerin (polimer FET'ler) çalışma voltajları 1 V'un altına düşürülmüştür. Polimer FET'lerin mikroakışkan kanala tümleştirilmesini kolaylaştırmak için, yeni bir düzlemsel OFET yapısı tasarlanmış ve tanıtılmıştır. Bu düzlemsel OFET'in çıkış karakteristiği üst-kapı alt-kontak bir OFET'inki ile karşılaştırıldığında, düzlemsel OFET'in yaklaşık 50 açma-kapama oranı sağlayarak, alan etkili transistör olarak başarı ile çalıştığı gösterilmiştir. Üst-kapı, alt-kontakt OFET yapısı için, döner-kaplama yöntemi ile P3HT filmi depolamanın damla-kaplama yöntemine göre daha yüksek açma-kapama oranına yol açtığı belirtilmiştir. Daha sonra, P3HT'nin mikrofabrikasyon işlemlerine dayanıklılığı incelenmiştir. Ayrıca, P3HT'nin NaCl ve KCl çözeltilerine duyarlılığı araştırılmıştır. Son olarak, polimer alan etkili transistörlerin üç farklı malzeme ile, polivinil alkol (PVA), parylene ve polidimetilsiloksan (PDMS), mikroakışkan kanallar ile kapsüllenmesi araştırılmıştır. Sıvı akışı sağlayan PVA mikroakışkan kanalları başarıyla oluşturulmuştur. Sırasıyla, açma ve kapama oranları 4 ve 10 olan düzlemsel polimer FET'ler parylene ve PDMS mikroakışkan kanallarına tümleştirilmiştir.

# TABLE OF CONTENTS

# LIST OF FIGURES

# LIST OF SYMBOLS

| | |
|---|---|
| C | Gate insulator capacitance per unit area |
| $g_m$ | Transconductance |
| $I_{Dsat}$ | Saturation drain current |
| $I_{DS}$ | Drain-source current |
| $I_{OFF}$ | Off current |
| $I_{ON}$ | On current |
| $L$ | Channel length |
| $V_{DS}$ | Drain-source voltage |
| $V_{GS}$ | Gate-source voltage |
| $W$ | Channel width |
| | |
| $\epsilon_0$ | Permittivity of vacuum |
| $\epsilon_r$ | Relative permittivity |
| $\mu$ | Carrier mobility |

# LIST OF ACRONYMS/ABBREVIATIONS

| | |
|---|---|
| a-Si | Amorphous Silicon |
| Au | Gold |
| CMOS | Complementary Metal-Oxide-Semiconductor |
| DI Water | Deionized Water |
| DL | Diffuse Layer |
| HL | Helmholtz Layer |
| HOMO | Highest Occupied Molecular Orbital |
| ISOFET | Ion Sensitive Organic Field Effect Transistor |
| LUMO | Lowest Unoccupied Molecular Orbital |
| MOSFET | Metal-Oxide-Semiconductor Field Effect Transistor |
| OECT | Organic Electrochemical Transistor |
| OFET | Organic Field Effect Transistor |
| OLED | Organic Light Emitting Diode |
| OSC | Organic Semiconductor |
| P3HT | Poly (3-hexyl thiophene) |
| PDMS | Polydimethylsiloxane |
| PVA | Polyvinyl Alcohol |
| rpm | Rotation per minute |
| RFID | Radio Frequency Identification |
| TCB | Trichlorobenzene |

# 1. INTRODUCTION

Discovery of first conducting polymer by Alan J. Heeger, Alan G. MacDiarmid, and Hideki Shirakawa in 1977 and the demonstration of both the first organic light emitting diode (OLED) by Ching W. Tang and Steven Van Slyke and the first organic field effect transistor (OFET) by H. Koezuka, A. Tsumura, T. Ando in 1980s resulted to a new research area called "organic electronics". Organic electronics is differentiated from inorganic electronics by using polymers and small molecules as semiconductors instead of inorganic semiconductor such as silicon. Even though organic electronics cannot replace single crystalline inorganic semiconductors in high speed and power circuits due to their lower stability and switching speed, organic field effect transistors (OFET's) now compete with amorphous silicon (a-Si) [2]. After intensive research, the mobility of polymeric semiconductor in OFETs is comparable to that of a-Si and the mobility of small molecule semiconductor in OFETs is close to that of poly-silicon devices [3]. Therefore, they are now intensely used in OLED display, organic photovoltaic cells and RFID tags.

Main advantages of organic electronics come from printability and flexibility of organic materials. They can be deposited and patterned at room temperature by printing and solution processes. Organic electronics provides the benefits of lower cost, usage of flexible substrates, large-area production over inorganic electronics [2]. One another important application of organic electronics can be chemical and biological sensing due to low-thermal budget processing techniques, compatibility with various substrates and changeable properties of organic materials [1, 4].

One of the critical problems that must be adressed is to reduce the operation voltage of OFETs in order to succeed low power consumption. Since organic semiconductors have moderate carrier mobility values, in order to get satisfactory conductivities below 1 V, gate capacitance should be increased [5]. This capacitance is governed by the gate insulator, which is one of the most important part of a field effect transistor. An ideal gate insulator must have a high dielectric constant and must be very thin.

Using electrolytes including ionic liquids, ion gels and even water as gate insulator meet these requirements in a simple and cheap way [6–8].

In this thesis, an OFET using a liquid electrolyte (DI water) as its gate insulator and poly (3-hexyl thiophene)(P3HT) as its polymeric semiconductor is realized and is utilized to sense analytes such as sodium and potassium ions in water and integrated into a microfluidic channel.

In Chapter 2, a basic review on organic field effect transistors is given. It concentrates on topologies and operation theory of OFETs, organic semiconductors and gate dielectrics used in OFETs, sensor applications and microfluidic channel integration of OFETs. Chapter 3 provides the fabrication and characterization part of the work together with the sensor results of newly proposed OFET structure. In Chapter 4, microchannel integration of OFET is presented with different fabrication techniques (bulk and surface micromachining) using different materials like polyvinyl alcohol (PVA), parylene and polydimethylsiloxane (PDMS). Finally, Chapter 5 presents conclusion and future work.

# 2. ORGANIC FIELD-EFFECT TRANSISTORS (OFETs)

## 2.1. OFET Structures

Organic field-effect transistors (OFETs) adopt the thin film transistor (TFT) structure where the semiconductor, the gate dielectric and the gate, source and drain electrodes are deposited as thin films. The substrate acts as a mechanical support and it has no function in the operation of OFETs.

There are four different structures of OFET. First distinction is based on where the gate electrode is positioned. When the gate electrode formation is the first or last step during fabrication, it is called as top-gate or bottom-gate, respectively. Second division arises from whether the source and drain electrodes are in contact with the semiconductor from bottom (bottom-contact) or top (top-contact). In this thesis, top gate, bottom-contact OFET structure as in Figure 2.1 is utilized. It has the advantage of being compatible with using liquid electrolytes as gate dielectrics and depositing semiconductor layer after formation of the source and drain electrodes.

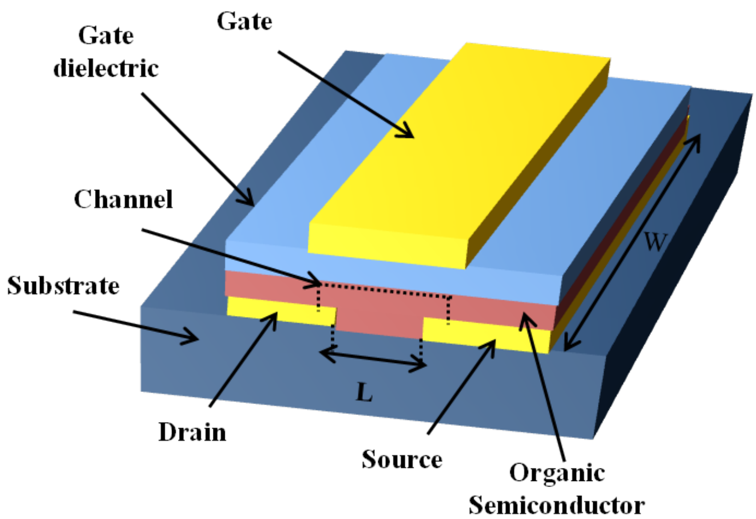


Figure 2.1. Top-gate, bottom-contact OFET structure.

## 2.2. Operation Theory and Characterization

Field-effect transistor utilizes a vertical electric field between the gate and the semiconductor to form a conducting channel between the source and drain electrodes. This electric field is generated between the capacitor plates, the gate electrode and the semiconductor, and the gate insulator is the dielectric of that capacitor. The capacitance per unit area can be found as defined by

$$C = \frac{\epsilon_r \epsilon_0}{d} \tag{2.1}$$

where d, $\epsilon_0$, $\epsilon_r$ are the dielectric thickness of the insulator, the permittivity of vacuum and the relative permittivity of the insulator, respectively.

When source electrode is grounded and the positive (negative) gate voltage ($V_{GS}$) is applied greater than the threshold voltage ($V_T$), negative (positive) charges accumulate in a very thin conducting channel. Here, $V_T$ is defined as the minimum sufficient gate voltage to form a conducting channel. Accumulation in a very thin layer due to the fact that the charge carriers are very closely localized to interface between the dielectric and the semiconductor [9]. When a potential difference ($V_{DS}$) is applied between drain and source electrodes, current ($I_{DS}$) starts to flow from the drain to the source or vice versa according to types of charge carriers.

Different from metal-oxide-semiconductor field-effect transistor (MOSFET), no depletion or inversion region exists in organic semiconductors for the isolation of active region from the substrate. When no gate voltage is applied, low off currents are guaranteed by very low amount of intrinsic charge carriers in organic semiconductors. Also, since there is no need to invert the charge carriers as in MOSFET, it operates only in the accumulation regime, not in inversion regime. Therefore, $V_T$ is not related to the strong inversion potential. It depends on the shallow traps that are closely packed in semiconductor surface and work function differences between gate and semiconductor [9, 10].

Like MOSFET, there are linear and saturation regimes for the operation of OFET as in Figure 2.2. While the source is grounded, if $|V_D| < |V_G - V_T|$, the transistor operates in linear regime and the current-voltage characteristics are governed by

$$I_{Dlin} = \frac{W}{L}\mu C\,[(\,V_G - V_T)V_D - \frac{V_D^2}{2}] \tag{2.2}$$

where W, L and $\mu$ are the channel width, the channel length and the carrier mobility, respectively.

On the other hand, if $V_D$ is increased such that $|V_D| \geqslant |V_G - V_T|$ , the transistor operates in saturation regime. The drain current is no longer $V_D$ dependent and determined by

$$I_{Dsat} = \frac{W}{2L}\mu C(V_G - V_T)^2 \tag{2.3}$$

In order to evaluate performance of OFETs, there are three significant characterization

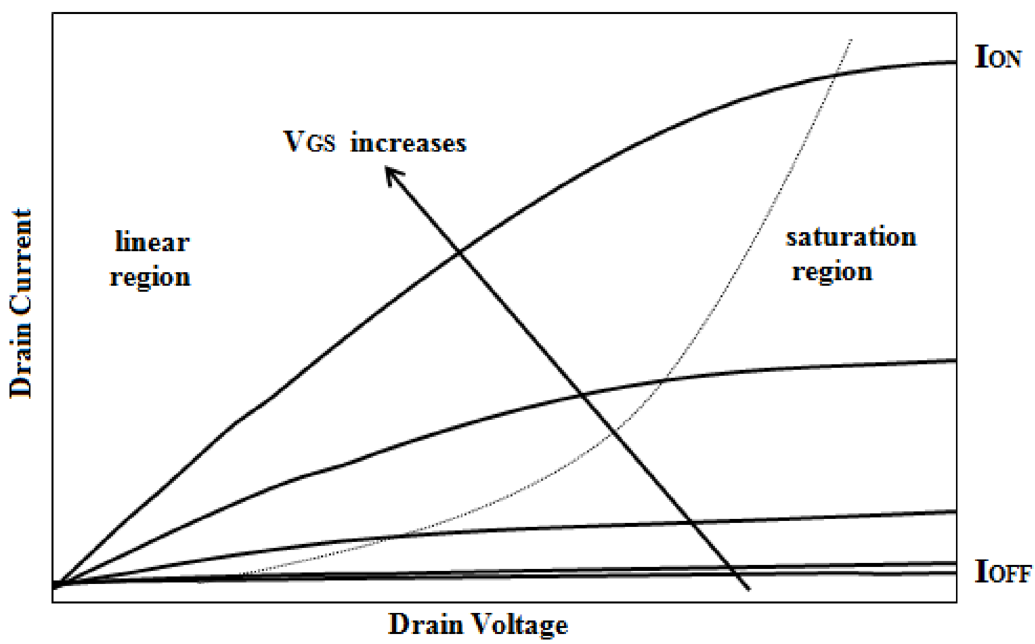


Figure 2.2. $I_{DS}$-$V_{DS}$ characteristics of a typical OFET.

parameters, the on-off ratio, the threshold voltage and the carrier mobility. The on-off ratio indicates how efficiently the drain current is modulated by $V_{GS}$. It is the ratio of the saturation current value when $V_{GS}$ is maximum (called on current) to the current when $V_{GS}$ is 0 (called off current since no channel is formed) and calculated by

$$\frac{I_{ON}}{I_{OFF}} = \frac{I_{Dsat}(V_{GS} = max)}{I_D(V_{GS} = 0)} \tag{2.4}$$

As another important parameter, the threshold voltage can be deduced from transfer characteristics of the OFET where the drain current versus the gate voltage for constant drain voltage is plotted as in Figure 2.3.

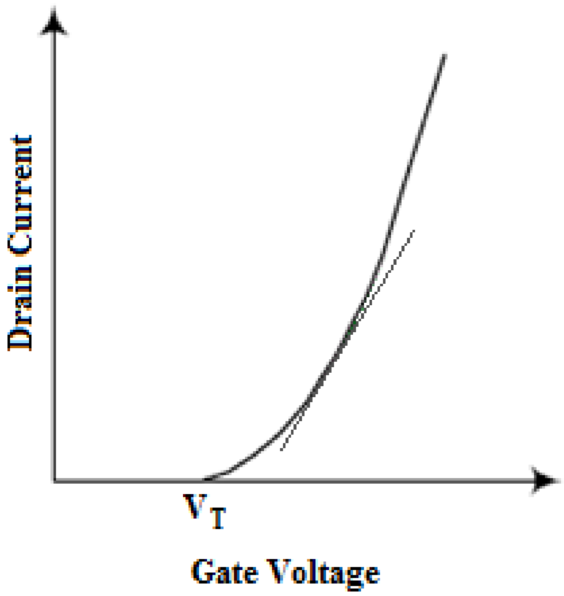


Figure 2.3. Transfer characteristics of a typical OFET.

Lastly, the carrier mobility can be calculated for both linear and saturation regimes. Linear carrier mobility can be calculated, first by extracting the transconductance, $g_m$, from Equation 2.2 as

$$g_m = \frac{\partial I_D}{\partial V_G} = \frac{W}{L}\mu C V_D \tag{2.5}$$

then, rearranging it

$$\mu_{lin} = \frac{Lg_m}{WCV_D} \tag{2.6}$$

As to saturation regime mobility, first the square root of Equation 2.3 is taken;

$$\sqrt{I_{Dsat}} = \sqrt{\frac{W\mu C}{2L}}(V_G - V_T) \tag{2.7}$$

and then from the slope of the $I_{Dsat} - V_G$ plot, it can be calculated.

## 2.3. Organic Semiconductors

Organic semiconductors comprise of mainly of carbon atoms. Although carbon has only two electrons available to bond in its ground state, exciting a 2s electron into the empty 2p orbital allows for four bonds. If the 2s orbital combines with the three 2p orbitals, four $sp^3$ hybridized orbitals form, yielding four single bonds with other atoms. These bonds are defined as $\sigma$-bonds and have highly localized electron density [11]. On the other hand, if the 2s orbital is mixed with only two of the three available 2p orbitals, $sp^2$ hybridization occurs. The three $sp^2$ orbitals form three $\sigma$-bonds whereas the remaining 2p orbital forms $\pi$-bond. Unlike $\sigma$-bonds, $\pi$-bonds have delocalized electron density and are responsible for the conductivity. If the 2s orbital is mixed with only one of the three available 2p orbitals, sp hybridization occurs.

The molecular orbitals split into bonding states called as HOMO (highest occupied molecular orbitals) and anti-bonding states known as LUMO (lowest unoccupied molecular orbital). They are analogous to valence and conduction bands in inorganic semiconductors.

### 2.3.1. Small Molecules and Polymers

Organic semiconductors divide into two classes according to molecular structures; small molecules and polymers. Small molecules have crystalline structures. They typically show hole mobilities in the range of 1-10 $cm^2/Vs$.The most explored examples of them are pentacene (Figure 2.4a) and rubrene (Figure 2.4b). Small molecules generally can be deposited by thermal evaporation in vacuum resulting in highly ordered and pure films [12]. Also, there are recent studies that realize solution-deposited pentacene film using precursor routes [13].

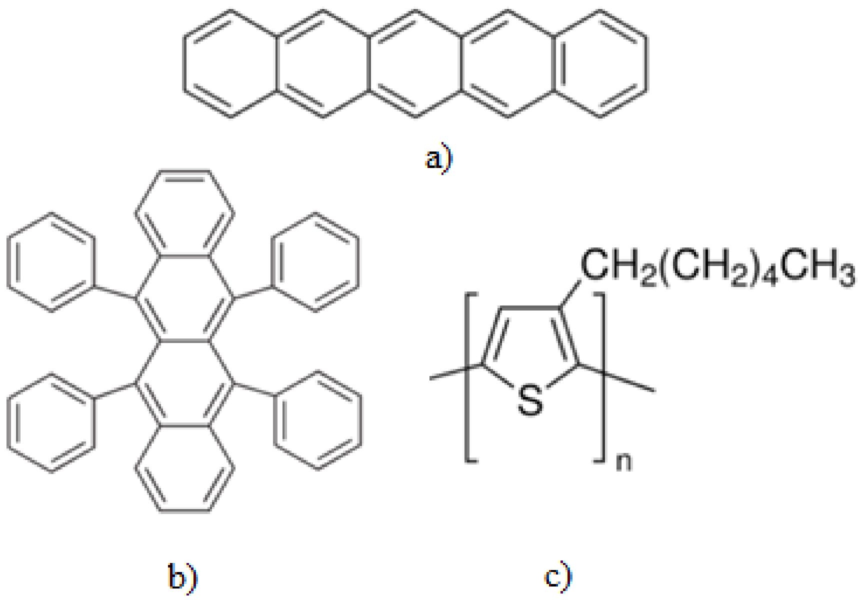


Figure 2.4. Molecular structures of (a) Pentacene, (b) Rubrene, (c) P3HT.

Polymeric semiconductors consist of a conjugated polymer backbone having an alternating sequence of single and double carbon bonds. They possess higher molecular weights and lower mobility values than small molecules. Currently, they may have mobilities up to 0.5 $cm^2/Vs$. Since they have good solubility in different solvents, they can be deposited by spin-coating or ink-jet printing leading to simpler and cheaper fabrication. The polymers cannot be deposited by thermal evaporation due to the fact that they cannot withstand to high temperatures in evaporation deposition.

The extensively used polymeric semiconductor, also the subject of this thesis, is poly(3-hexylthiophene) (P3HT) as given in Figure 2.4c due to its high carrier mobility and being solution-processible. It consists of thiophene ring backbone to which a hexyl side chain is added. Hexyl side chain makes the polymer soluble in organic solvents. On the other hand, it has poor air stability, but still it is one of the most stable semiconductor polymer at room conditions [14].

Mobility of P3HT is affected by several factors such as regioregularity, the solvent type and molecular weight. Regioregularity means the proportion of head to tail linkages between monomers. High regioregular P3HT shows high carrier mobilities exhibiting high ordered film structure. The usually employed solvents are chloroform, xylene and trichlorobenzene (TCB). Although high boiling point solvents lead to more microcrystalline structures and higher carrier mobilities, the chloroform is the most studied one, also for this thesis, because it dissolves P3HT more easily than xylene and evaporates more rapidly than TCB [15]. In addition, higher molecular weights of P3HT lead to higher carrier mobilities. That can be explained by the grain boundaries between the crystallites or disordered backbone conformation in low molecular weights of P3HT [16, 17].

### 2.3.2. P-type and N-type Organic Semiconductors

Organic semiconductors can also be referred as n-type or p-type depending on the type of conduction carriers. The above mentioned materials are p-type organic semiconductors meaning that holes are transported through the channel. On the other side, n-type organic semiconductors exhibit electron transport. Fullerene-based materials like $C_{60}$ reside in n-type organic semiconductors [18]. They generally show low electron mobilities because of electron trapping at dielectric-semiconductor surfaces and insufficient electron injection. That is why they are less intensively explored than p-type organic semiconductors despite of the fact that they are necessary for complementary logic circuits as in CMOS.

Electron conduction is very limited in semiconducting polymers since electron trapping at the semiconductor-dielectric interface such as $SiO_2$ is usual [19]. In addition, since the source and drain electrodes inject charge carriers to organic semiconductor or retrieve them from it, they constitute barriers to electron injection since they are usually made of high work function metals. This is related to forming an ohmic contact between the semiconductor and the source and drain electrodes. However, due to the ionization potentials of p-type organic semiconductors, gold is a good choice for the electrodes [4]. Also, formation of gold electrodes is easy. However, in order to promote electron transport in organic semiconductors, electrodes should have an accessible low energy LUMO meaning a low work function such as calcium (Ca) [18]. However, forming electrodes from these metals such as calcium is not straightforward since they react and get oxidized readily at room conditions. On the other hand, there are recent researches showing ambipolar property of organic semiconductors exhibiting both electron and hole conduction conforming to gate bias direction [2].

### 2.3.3. Charge Transport

Charge transport occurs by band transport in inorganic semiconductors whereas it is generally explained by hopping mechanism in polymeric semiconductors. This model bases on hopping of charges between localized states. After a charge carrier hops, it leads to a local deformation of the polymer called polaron. Since hopping mechanism needs lattice vibrations, it is phonon-assisted and the charge mobility increases with temperature in polymeric semiconductors [12].

Other charge transport explanation is based on multiple trapping and release model. In that model, charge transport occurs by band transport but now they can be trapped from impurities and defects. After a certain time, they can be released by thermal activation. This model is usually utilized to explain charge transport in small molecules [20].

## 2.4. Gate Insulators in OFETs

### 2.4.1. Classical Dielectrics

At the beginning, organic electronics started to use thermally grown $SiO_2$ as gate insulator as an inheritance from inorganic electronics. Polymer field-effect transistors employing $SiO_2$ ($\epsilon_r$=3.9) with thickness of 200 nm typically requires gate voltages of -40 V [21]. In order to reduce operating gate voltages, gate dielectric capacitance should be increased. This can be achieved by decreasing dielectric thickness or using materials having high dielectric constant. Therefore, the high dielectric constant materials like tantalum oxide ($\epsilon_r$=21) with thickness of 100 nm and titanium oxide ($\epsilon_r$=41) with thickness of 97 nm are used in OFETs [22, 23]. In addition, organic dielectrics can also be utilized as gate dielectric. Low voltage operation are succeeded using poly-4vinylphenol ($\epsilon_r$=6) with thickness of 20 nm and polyvinyl alcohol (PVA) with thickness of 9 nm [24, 25].

### 2.4.2. Electrolytes

Recently, there has been a great tendency to use electrolytes as gate insulator in OFETs in order to provide low voltage operation below 1 V, utilizing the formation of electrical double layers between solid and electrolyte interfaces as explained in Section 2.5. Electrolytes can be solid or liquid. One type of solid electrolytes used in OFETs is polymer electrolyte. The example is polyethylene oxide containing a Li salt [26]. The main disadvantage of solid electrolytes is lower switching speeds since ionic migration in them is limited [5]. On the other hand, liquid electrolytes include ionic liquids, ion gels and electrolyte solutions. Ionic liquids are completely salts in liquid state at room temperature [27]. As to ionic gels, they consist of an ionic liquid and a block copolymer [7]. Finally, electrolyte solutions are formed when a salt is dissolved in a solvent such as water.

### 2.5. Electrical Double Layer Capacitance

When electrolytes are used as gate dielectrics in OFETs, electrical double layers are generated on the gate electrode-electrolyte and electrolyte-semiconductor interfaces. These electrical double layers have quite high capacitance values about a few tens of $\mu F/cm^2$ resulting to decrease in operation voltages of OFETs.

In Figure 2.5, the combined Gouy-Chapman-Stern model of the electrical double layer can be seen. For example, when the gate electrode is negatively biased, positive ions (cations) in the electrolyte move to the gate-electrolyte interface whereas repelled negative ions (anions) move to the electrolyte-semiconductor interface. The first layer from the surface, called Helmholtz layer, includes the single layer of ions which are charged oppositely to the surface charges. The next layer through the electrolyte is called as diffuse layer since it consists of oppositely charged ions diffusing into the interface. In the diffuse layer, the concentration of the oppositely charged ions decreases gradually through the bulk [1].

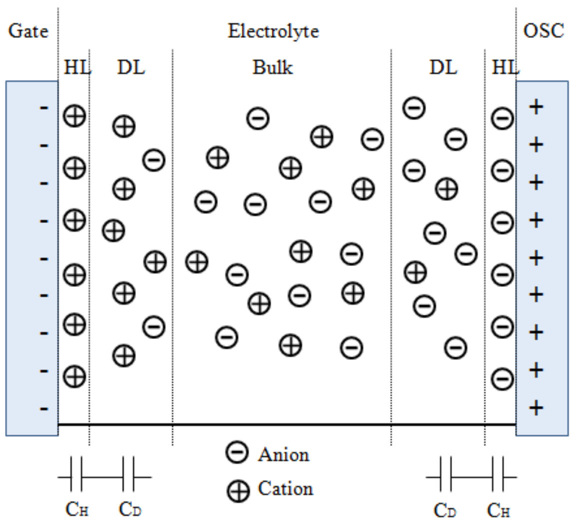


Figure 2.5. Electrical double layers between gate-electrolyte and electrolyte-organic semiconductor (OSC) interfaces according to Gouy-Chapman-Stern model showing the Helmholtz layer (HL), diffuse layer (DL) and equivalent capacitance model [1].

The total capacitance can be modeled as the series combination of Helmholtz layer and diffuse layer capacitances. Thus, it is determined by the smaller of them which is diffuse layer capacitance at low electrolyte concentration. When the electrolyte concentration increases, the diffuse layer thickness decreases leading to increase in diffuse layer capacitance. As the electrolyte concentration further increases, the total capacitance is not only determined by diffuse layer capacitance only but starts to get notable contributions from the Helmholtz layer capacitance [28]. As seen, the total capacitance has nothing to do with electrolyte thickness [29].

## 2.6. Sensor Applications

Organic thin film transistors are also studied as chemical or biological sensors. Especially, disposable biosensors are the possible applications area of these devices. For sensor applications, there can be four different detection structures of organic thin film transistors as seen in Figure 2.6.

In Figure 2.6a, there is a classical bottom-gate/top-contact OFET in which current is modulated by the influence of the analyte on the grain boundaries and the change in number of traps in the organic semiconductor [1]. Since organic semiconductors are normally affected by the moisture and oxygen in the ambient environment, these effects have to be considered carefully.

As to Figure 2.6b, an ion-sensitive OFET topology (ISOFET) utilizing the change in the characteristics of gate dielectric-electrolyte interface is seen. In this implementation, an electrolyte is formed over the gate insulator and the contact is taken from this electrolyte by means of a gate electrode. The binding of the ions on the electrolyte to the gate insulator results to the changes in the threshold voltage of organic field-effect transistor. Making the gate dielectric sensitive to specific analytes may increase the selectivity of sensors.

In Figure 2.6c, there exists an electrolyte gated OFET. In this architecture, the electrolyte serves as gate insulator. There is no electrochemical reaction between electrolyte and organic semiconductor. Electrical double layer forms between them. This

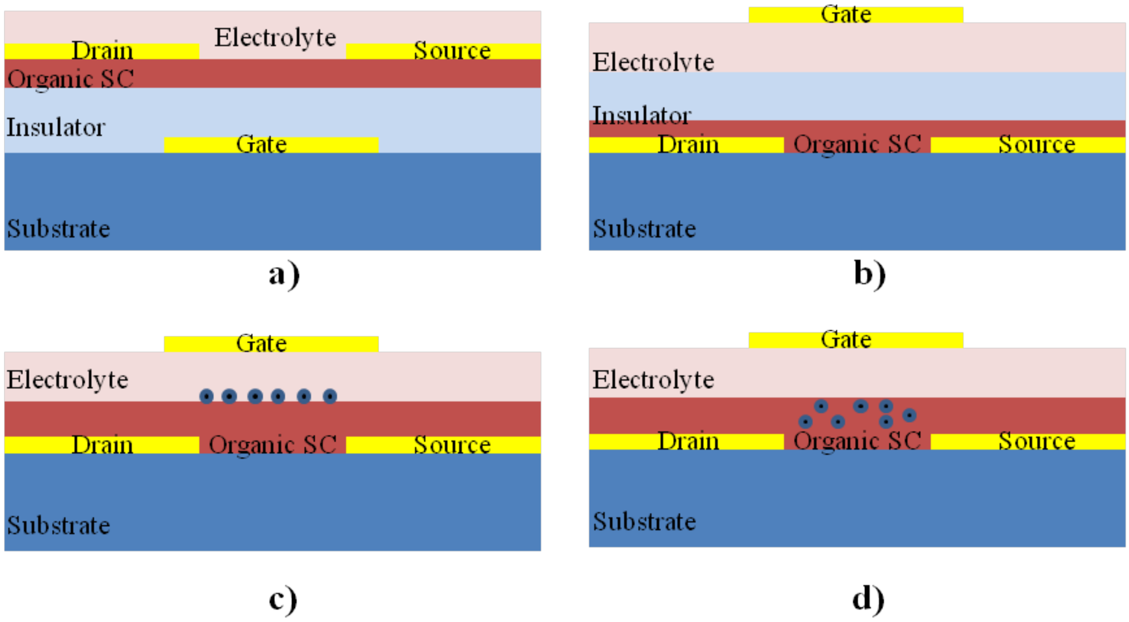


Figure 2.6. (a) OFET operating in electrolyte, (b) An ion-sensitive OFET (ISOFET), (c) An electrolyte gated OFET, (d) Organic electrochemical transistor (OECT).

electrical double layer creates high electric field, which modulates the charge carriers only close to interface and prohibits electrical current through the interface. However, if there is electrochemical reaction between electrolyte and organic semiconductor, this architecture turns into organic electrochemical transistor (OECT) as given in Figure 2.6d [26]. Since the electrolyte is directly in contact with active organic semiconductor, semiconductor can be doped or de-doped and that change modulates the current. But, ion penetration disturbing the crystalline structure of organic semiconductor can result to degradation in performance of OFETs. Electrochemical doping can also happen in electrolyte gated OFETs. However, in terms of output characteristics, clear saturation effect and square law behavior are the marks of the field-effect operation [5].

## 2.7. Microfluidic Channel Integration

For the sensor applications of liquid electrolyte-gated OFETs, it is important to confine the liquid to a microfluidic channel by capillary forces. Such an encapsulation provides the advantages of low permeability to water and oxygen, same area of active region for each sensor, more reliable and consistent results. In that sense, microfluidic channels are passive such that there is no manipulation of liquid [30]. This hybrid integration combine liquid and electronic on the same chip.

Figure 2.7 shows top and cross-sectional views of conceptual design of an OFET integrated into the microfluidic channel. The gate electrode is located at the ceiling of the microfluidic channel whereas the source and drain electrodes are placed at the floor. Polymer semiconductor completely covers over the source and drain electrodes and gate insulator becomes the liquid inside the microfluidic channel. Reservoirs should be opened in microfluidic channels to provide the entry and exit to the liquid. Chapter 4 gives detailed integration process with different microfluidic channel materials like PDMS, PVA and parylene.

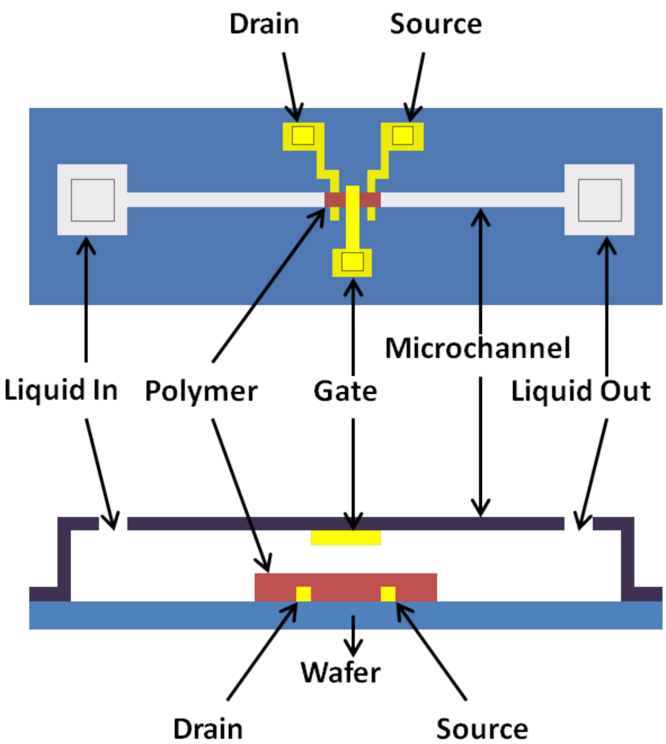


Figure 2.7. Top and cross-sectional views of liquid electrolyte gated organic field-effect transistor integrated into a microfluidic channel.

# 3. FABRICATION AND CHARACTERIZATION

## 3.1. Device Design

There are two different organic field effect transistor topologies that use DI water as their gate electrolytes, studied in this thesis, as seen in Figure 3.1. They are differentiated according to gate electrode location. Since it is hard to form gate electrode physically over active region, the first topology uses a probe as the gate electrode for simplicity [10]. However, consistent probe location and area cannot be achieved in this method. For further possible research on sensor applications of this device, liquid electrolyte should be confined to a microfluidic channel [30]. It is a considerable challenge to integrate this vertical gate electrode to the ceiling of the microfluidic channel. In order to overcome this difficulty, a novel OFET topology using a planar gate electrode is tested as shown in Figure 3.1 where gate probe is not used. It is called planar OFET because gate electrode is in the same plane with drain-source electrodes. The

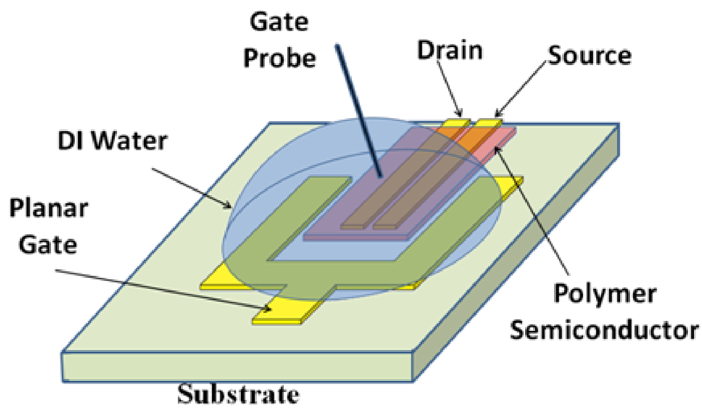


Figure 3.1. Two different topologies of water gate polymer field effect transistor with gate electrode being either gate probe or planar gate while the other is floating.

main advantage comes from the fact that both gate electrode and source-drain electrodes are formed and patterned on the same plane at the same time. It is critical to form the polymer semiconductor over only source-drain electrodes, not touching to the gate electrode. Also, electrolyte should only touch to the gate electrode and does not touch to source-drain electrodes. Since electrical double layer over the active region is generated, the carriers accumulate at this region and channel is formed.

According to the structures of the source and drain electrodes, two different mask types of single electrode (left) and interdigitated electrodes (right) as shown in Figure 3.2 are designed. For the single one, the device has length of 4 $\mu$m and width of 600 $\mu$m and gate electrodes are separated from the source-drain electrodes with a gap of 500 $\mu$m. As to interdigitated one, the device length is same whereas width is 7 times the single structure and gate electrodes are separated from the source-drain electrodes with a gap of 300 $\mu$m. The microfluidic channel has width of 200 $\mu$m and length of 5 mm in both designs. Sacrificial photoresist mask of polymer semiconductor is 100 $\mu$m wider than microfluidic channel due to possible alignment errors.

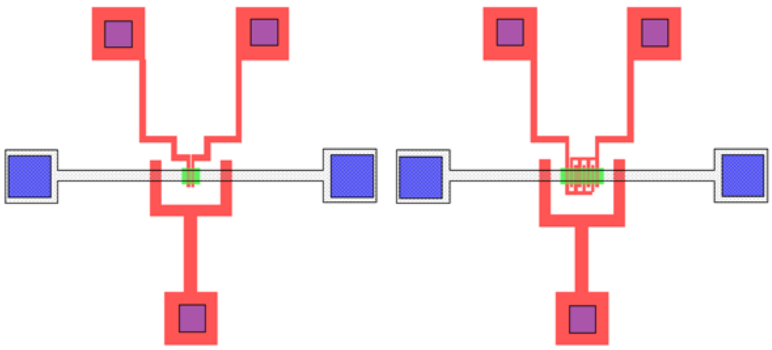

Figure 3.2. Two different designed masks for both single (left) and interdigitated (right) electrodes. The colors of red, green, white, blue show different masks for electrodes, polymer, microchannel and reservoirs, respectively.

### 3.2. Device Fabrication

To fabricate the devices, firstly Shipley 1805 positive photoresist is spin-coated at 2000 rpm over Cr-Au coated glass wafer. After soft baking at 90 $^oC$ for 1 minute, wafer is exposed to UV light at 490 Watts (Figure 3.3) for 40 seconds and developed at MF24A for 1 minute. After photoresist is patterned, gold is etched and photoresist is removed in acetone before removing chrome since there is a chemical reaction between chrome etchant and photoresist. Finally, chrome is etched. Then, the wafer is cleaned in acetone, isopropyl alcohol and DI water, respectively. Figure 3.4 shows the microscope images of patterned single (left) and interdigitated (right) electrodes.

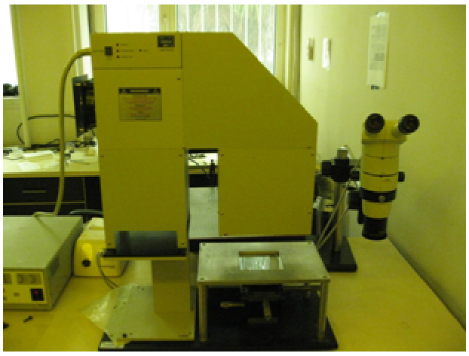

Figure 3.3. Newport UV light exposure source and mask aligner system.

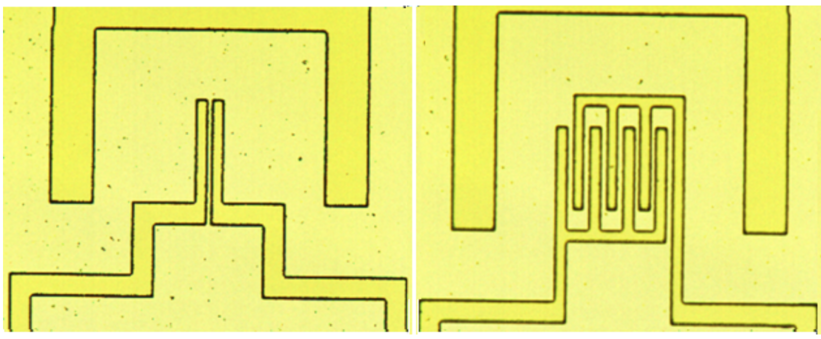

Figure 3.4. The microscope images of patterned single (left) and interdigitated (right) electrodes.

Polymeric semiconductor used in the experiments are prepared from P3HT (%95 regioregular) purchased from Sigma-Aldrich Co. It is dissolved in chloroform at 40 $^{o}$C for 2 hours resulting to concentration of 2 mg/ml.

### 3.3. Device Characterization

Manufactured devices are characterized by using Keithley 4200-SCS semiconductor characterization system and hand-made probe station as shown in Figure 3.5. $I_{DS}$-$V_{DS}$ characteristics are taken while $V_{DS}$ is changing from 0 to -0.5 V with 0.02 V steps and $V_{GS}$ is changing from 0 to -1 V with 0.25 V steps where source electrode is grounded.

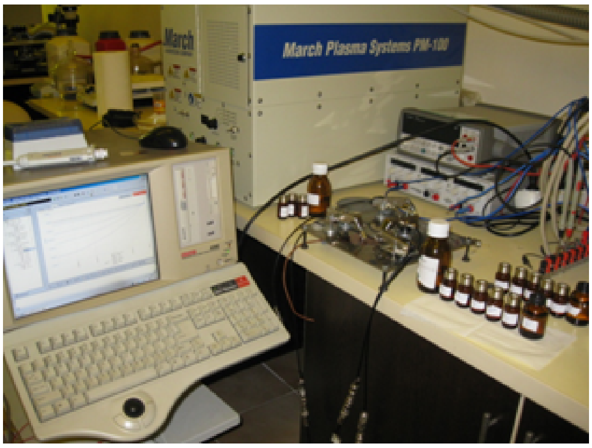


Figure 3.5. Keithley 4200-SCS semiconductor characterization system and probe station.

### 3.3.1. Drop Casting

After electrodes are formed over glass wafer as in Figure 3.6 (left), to test if they are working like field effect transistor, test setup in Figure 3.6 (right) is prepared. After P3HT is fully deposited over device with drop-casting, the connection between the gate electrode and P3HT is carefully cut under the microscope. Then, a droplet of DI water as gate electrolyte is put over the P3HT film covering both the P3HT film over drain-source electrodes and gate electrode.

$I_{DS}$-$V_{DS}$ characteristics of single electrode devices can be seen in Figure 3.7 for both gate probe and planar gate topologies. For planar OFET, at $V_{DS}$=-0.5V, $I_{OFF}$ ($V_{GS}$=0V) is 4.3 nA and $I_{ON}$ ($V_{GS}$=-1V) is 144 nA, leading to on-off ratio of about 33. As to gate probe OFET, $I_{OFF}$ and $I_{ON}$ are 2.8 nA and 136 nA, respectively, resulting to on-off ratio of about 49.

$I_{DS}$-$V_{DS}$ characteristics of interdigitated electrode devices can be seen in Figure 3.8 for both gate probe and planar gate topologies. For planar OFET, $I_{OFF}$ and $I_{ON}$

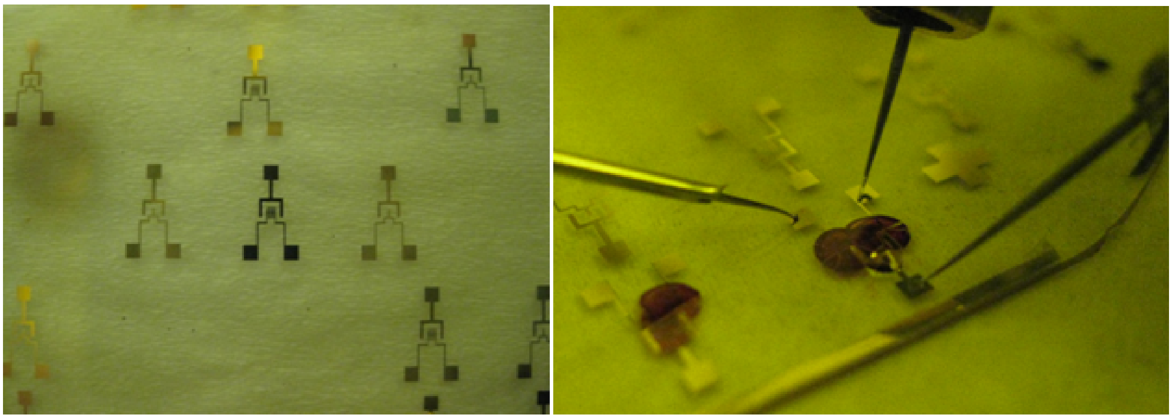

Figure 3.6. Photograph of fabricated devices before testing (left) and during testing (right).

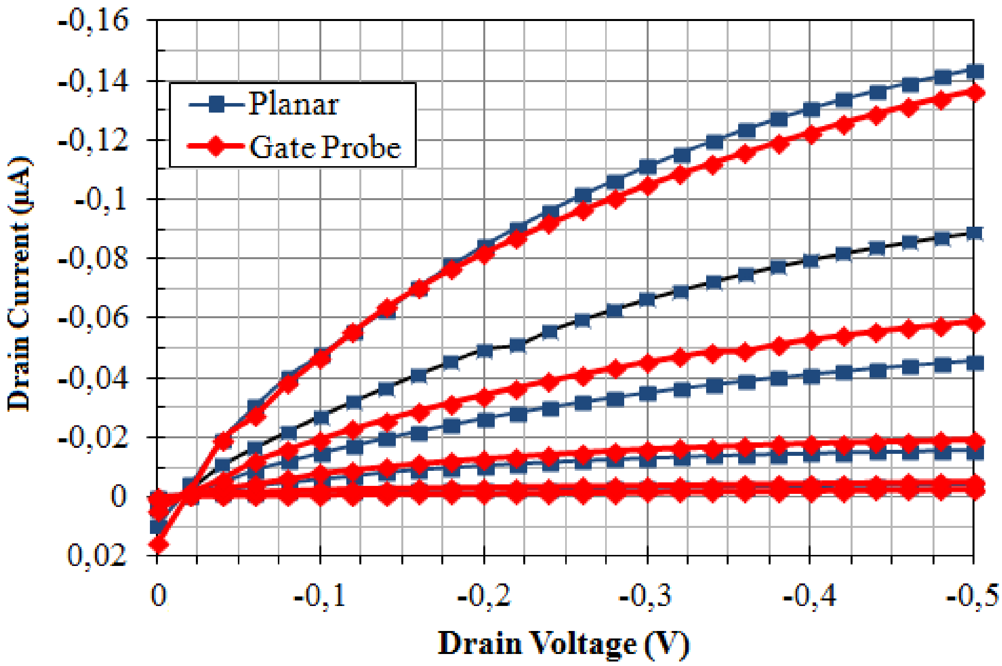


Figure 3.7. $I_{DS}$-$V_{DS}$ characteristics of single electrode devices for both gate probe and planar gate topologies where P3HT film is deposited by drop-casting.

are 25 nA and 380 nA, respectively, leading to on-off ratio of about 15, whereas for gate probe OFET, they are 14 nA and 334 nA, resulting to on-off ratio of about 24. It is clear that for both topologies, $I_{ON}$ increases by about 2.5 times for the interdigitated electrode devices. On the other hand, $I_{OFF}$ increases more than 2.5 times leading to decrease in the on-off ratio. This is probably resulted from the fact that the increase in active region of the transistor adds to the defects in the film morphology.

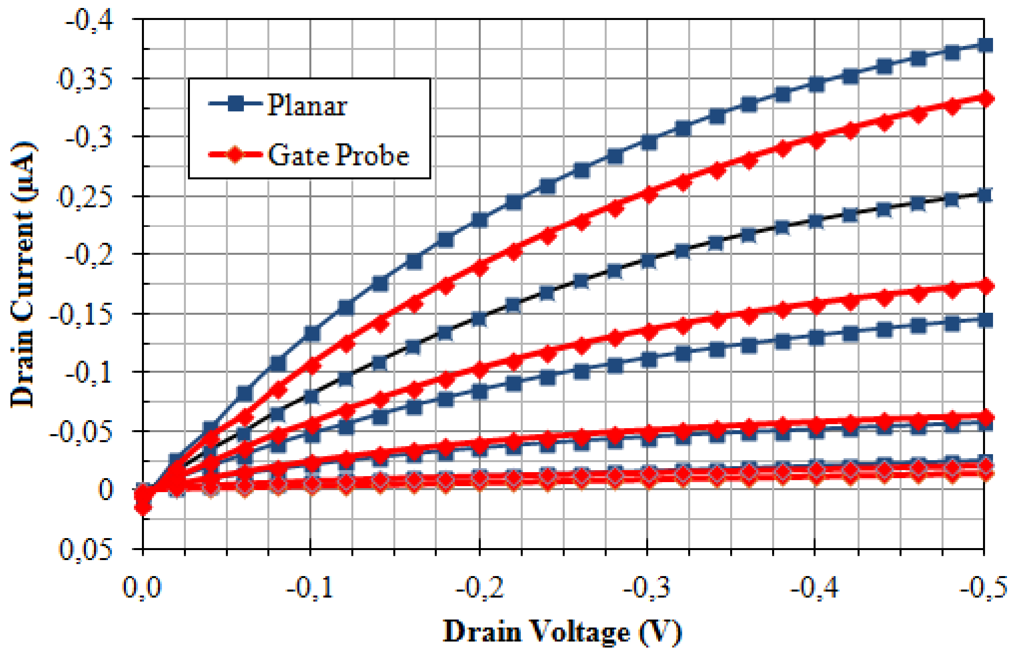


Figure 3.8. $I_{DS}$-$V_{DS}$ characteristics of interdigitated electrode devices for both gate probe and planar gate topologies where P3HT is deposited by drop-casting.

When the gate probe and planar gate topologies are compared, it is seen that planar gate one provides similar output characteristics to gate probe one. Therefore, it ensured that newly proposed OFET structure successfully operates as a field effect transistor providing the square law and showing the saturation behavior.

### 3.3.2. Spin Coating

The microfabrication steps during integration of OFET to microfluidic channel decrease the mobility of P3HT. Before patterning the P3HT, it is important to optimize maximum on current and on-off ratio to be able to obtain a working OFET after microfabrication steps. Therefore, it is investigated whether the deposition of P3HT film by spin-coating results to higher mobility values than using drop-casting method by forming a regular film. In this case, P3HT solution is spin-coated by first pouring it over the wafer and then immediately spinning the wafer at 2000 rpm.

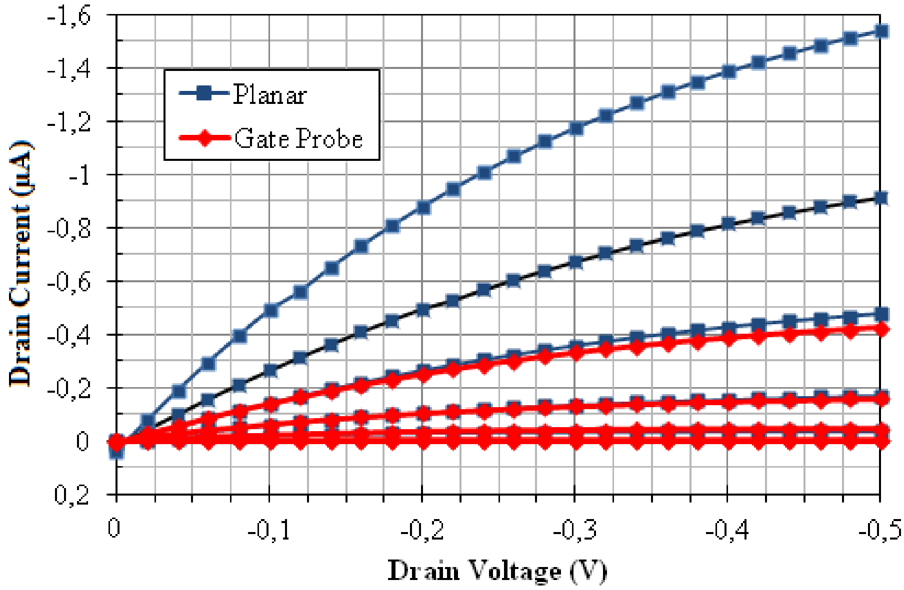


Figure 3.9. $I_{DS}$-$V_{DS}$ characteristics of single electrode devices for both gate probe and planar gate topologies where P3HT film is deposited by by spin-coating.

Figure 3.9 and Figure 3.10 shows the output characteristics of single and interdigitated electrode devices, respectively, where P3HT is spin-coated. For single electrode planar OFET, $I_{OFF}$ and $I_{ON}$ are 36 nA and 1.54 $\mu$A, respectively, leading to on-off ratio of about 49, whereas for single electrode gate probe OFET, they are 1.97 nA and 425 nA, resulting to on-off ratio of about 215. As to interdigitated electrodes, planar OFET has $I_{OFF}$, $I_{ON}$ and on-off ratio values of 277 nA, 26 $\mu$A and about 94, respectively, whereas for gate probe OFET, they are 22.6 nA, 12.4 $\mu$A and about 548. As compared to drop-casting P3HT, spin-coating results to much higher on currents and on-off ratio.

In the literature, it is claimed that drop casting gives better mobility values than

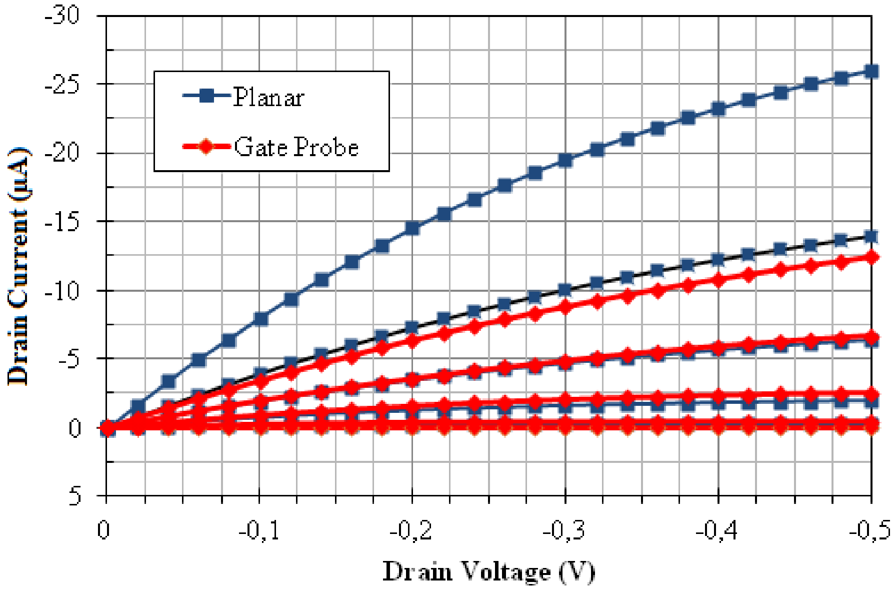


Figure 3.10. $I_{DS}$-$V_{DS}$ characteristics of interdigitated electrode devices for both gate probe and planar gate topologies where P3HT is deposited by by spin-coating.

spin-coating due to slower evaporation time of the solvent resulting to more ordered film structure [21]. As seen, it is contrary to the findings given in Figure 3.7 and Figure 3.9. This can be originated from the gate location. The research in the literature focuses on the bottom-gate structure with $SiO_2$ gate dielectric over which source and drain electrodes and polymer semiconductor is deposited. So, active region in the polymer semiconductor is its bottom part contact with $SiO_2$. In contrast, when top gate topology is used, active region is the upper part of the semiconductor. Thus, the fact that spin-coating leads more regular morphology than drop-casting for top of the film explains the ambiguity.

### 3.4. Patterning of P3HT

The critical point in this device fabrication is to cut the contact between polymer semiconductor and gate electrode. Since it is challenging to scratch the polymer in each device for a batch fabrication, patterning the polymer semiconductor film by lithography is considered. To be able to observe the effect of patterning on polymer semiconductor, two different photoresists; SPR220.07 and PR1828 are used in experiments. The process flow to pattern P3HT is described in detail in Figure 3.11. Firstly, P3HT is spin-coated over the clean wafer. Then, photoresist (SPR220.07 or PR1828) is deposited over P3HT film by spin-coating and patterned by photolithography according to its recipe as given in Appendix A and Appendix B, respectively. The residual P3HT is removed by oxygen plasma etching using March oxygen plasma cleaner in Figure 3.12 . Finally, protective photoresist is removed in acetone.

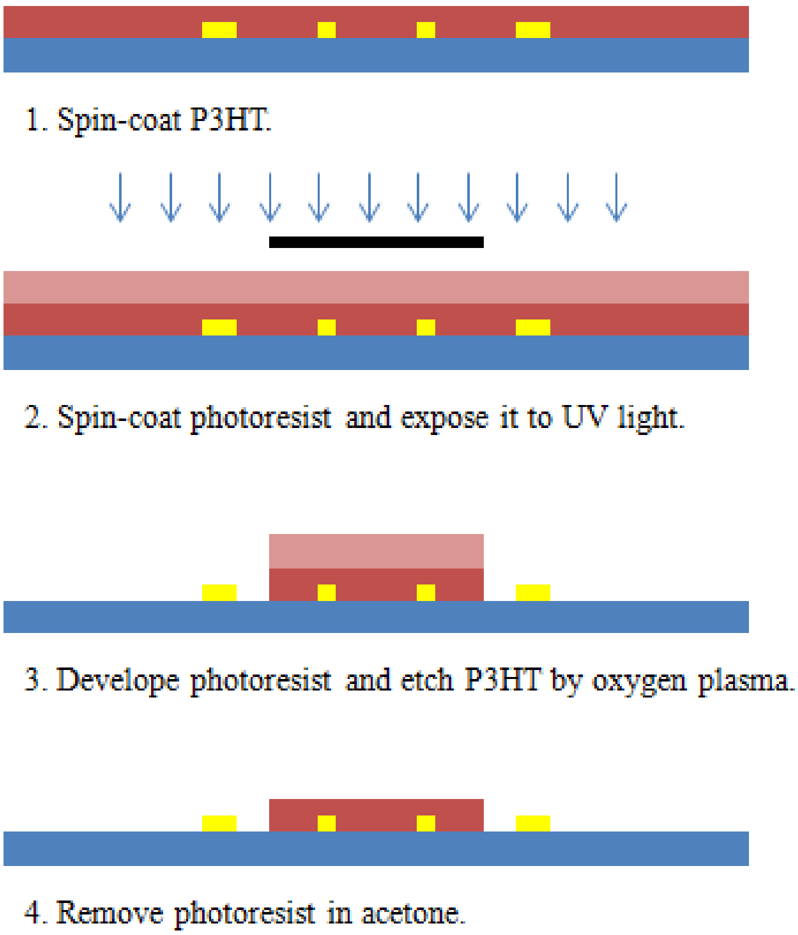


Figure 3.11. Process flow of P3HT patterning.

If photoresist is patterned immediately after P3HT film is spin-coated, it is seen that electrical characteristics of device completely disappear. This probably originates from the chemical reactions between the solvent of P3HT and photoresist since the solvent of P3HT is not completely dried. To solve this problem, P3HT film is annealed


Figure 3.12. March oxygen plasma cleaner.

at 70 $^{o}$C for 1.5 hours under the vacuum after it is spin-coated. So, it is guaranteed that the residual solvent completely evaporates. Figure 3.13 shows the patterned P3HT film over planar OFET.

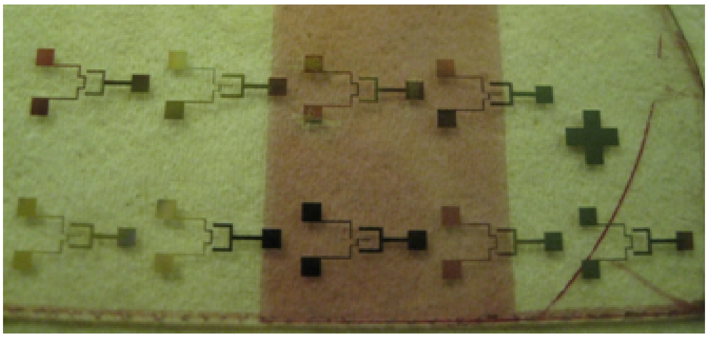

Figure 3.13. Patterned P3HT over planar OFET.

Figure 3.14 and Figure 3.15 shows the output characteristics after P3HT is patterned by PR1828 and SPR220.07, respectively. When the results are compared, it is obvious that there is a decrease in $I_{ON}$ and on-off ratio for each photoresist after patterning although PR1828 protects the polymer more than SPR220.07. This is probably due to less heat treatment done during patterning process. Nevertheless, both devices successfully operate as field effect transistor. The potential causes for the decrease in performance are stress resulted from the different thermal coefficients of photoresist and P3HT during the heating for photolithography, effect of UV light and acetone [31].

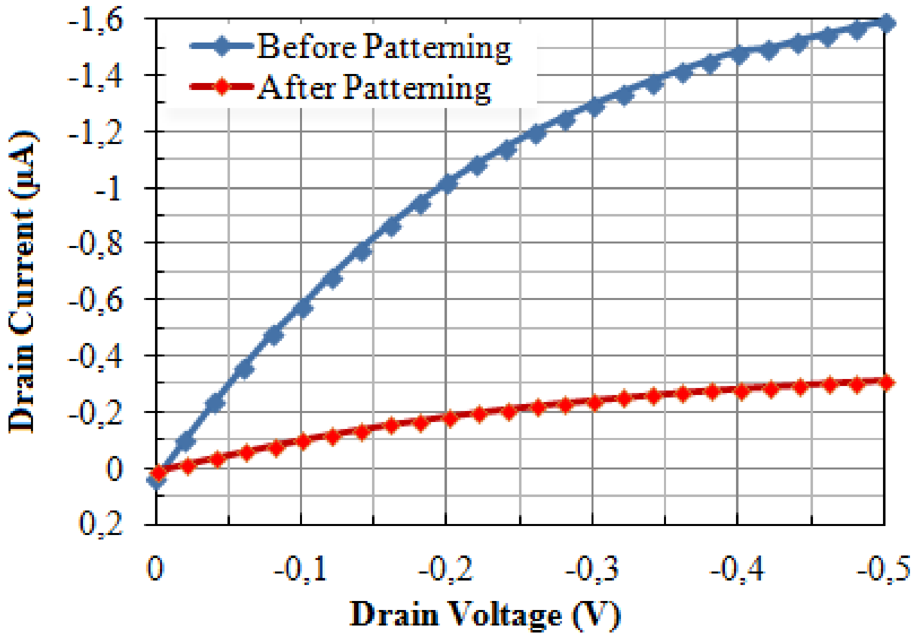


Figure 3.14. Effect of patterning P3HT with PR1828 on $I_{ON}$ values.

### 3.5. Acetone Duration of P3HT

After microfluidic channel is formed and its reservoirs are opened, to remove the sacrificial photoresist layer and open the microfluidic channel completely, devices should be kept at acetone about 1 or 2 days. In order to determine the effect of acetone on P3HT, first of all P3HT is spin-coated over the planar OFET and left at 70 $^oC$ for 1.5 hours under vacuum. Then the device is left into acetone and $I_{DS}$-$V_{DS}$ characteristics are taken every 24 hours. $I_{ON}$ values of two different devices can be seen on Figure 3.16. As seen, $I_{ON}$ decreases to some extent for the first 24 hours and then stays nearly constant for the next 24 hours. Another work in the literature indicates similar results [32]. However, the devices continue to operate as field effect transistor.

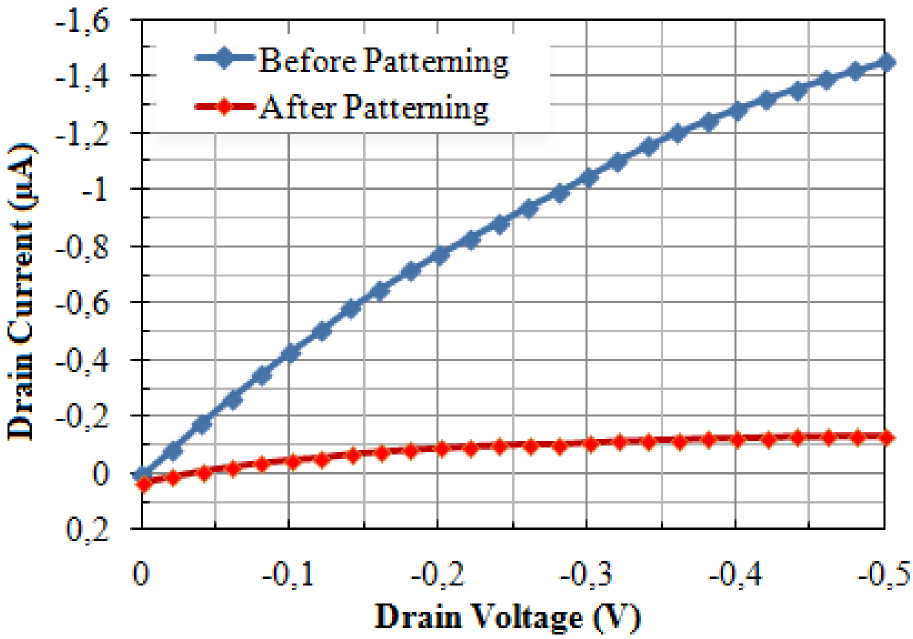


Figure 3.15. Effect of patterning P3HT with SPR220.07 on $I_{ON}$ values.

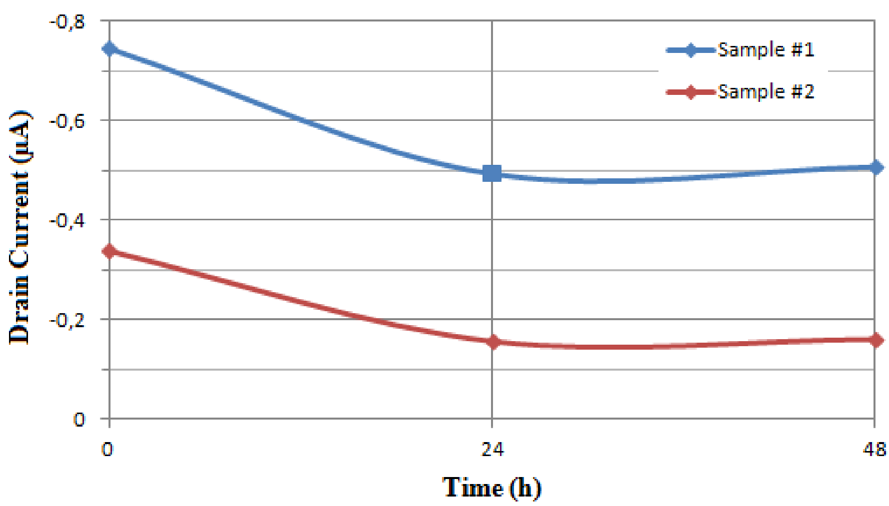


Figure 3.16. $I_{ON}$ values of OFET left in acetone versus time for two different samples.

### 3.6. Sensing Capability of P3HT

The sensitivity of P3HT with respect to NaCl and KCl is also researched using the planar gate topology. Figure 3.17 and Figure 3.18 shows the on current values of single electrode devices with changing salt concentration of NaCl and KCl, respectively. For both salt solutions, drain current decreases with increasing concentration first, However, then it increases. The initial decrease with solution concentration can be explained by electrochemical doping. The later increasing current with increasing salt concentration can be sourced from the increase in electrical double layer capacitance. The same tendency for both salts reveals that P3HT does not have selectivity to these salts. Therefore, it is compulsory to functionalize the P3HT for specific analytes for further sensor applications. In addition, it is hard to obtain an exact analysis due to the difficulties in separating the salt concentration effect from the environmental effects. Therefore, it is another necessity to encapsulate the device by integrating it into a microfluidic channel.

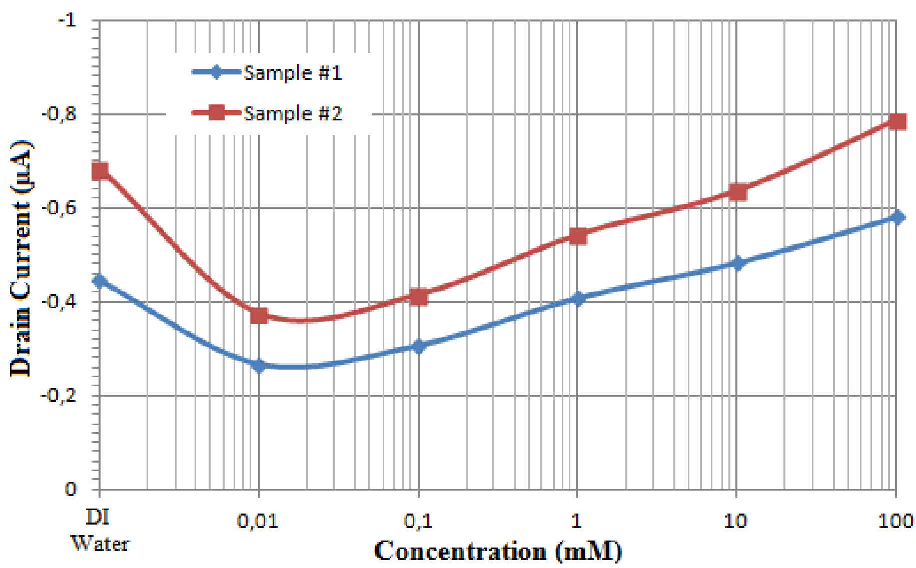


Figure 3.17. $I_{ON}$ values of OFET subjected to different concentration of NaCl solution for two different samples.

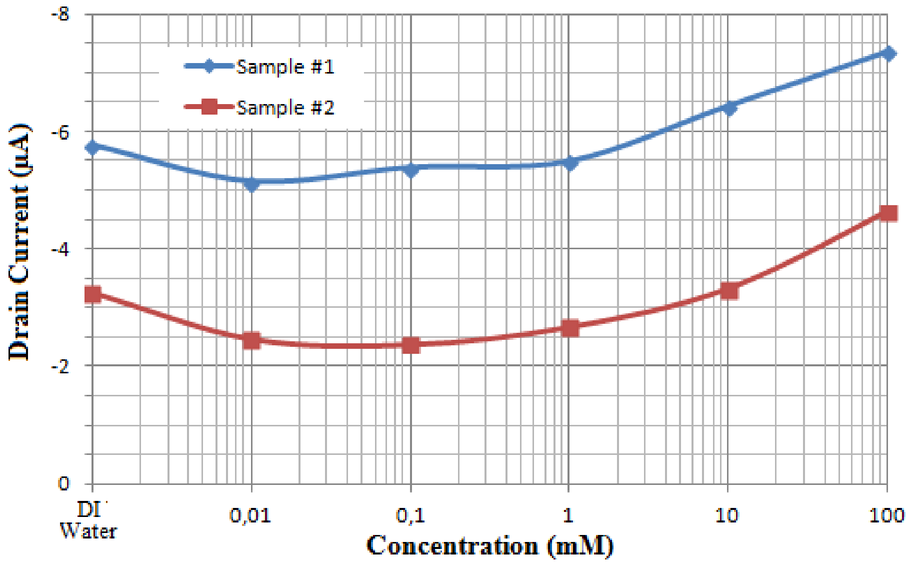


Figure 3.18. $I_{ON}$ values of OFET subjected to different concentration of KCl solution for two different samples.

# 4. MICROCHANNEL INTEGRATION

During integration of the electrical double layer capacitance OFET to the microfluidic channel, it is very troublesome to form gate electrode over source and drain electrodes in the vertical plane. That results from high possibility of the collapsing of the gate electrode. Also, it requires additional process steps leading to more deterioration of polymer semiconductor. Therefore, it is not practical to realize conceptual design as in Section 2.6. Therefore, a new integration process flow is designed as compatible with planar OFET.

## 4.1. Integration Process Flow of Parylene and PVA

To integrate planar OFET to the microfluidic channel, process flow as shown in Figure 4.1 can be followed, respectively. First of all, electrodes are formed over glass wafer. Then, P3HT is spin-coated and patterned. Thick sacrificial photoresist is patterned and residual P3HT is removed by oxygen plasma in 2 minutes. And either PVA or parylene is deposited in order to form channel walls. Thick photoresist is spin-coated and patterned with the aim of protecting the microfluidic channels during etching the reservoirs. Lastly, the reservoirs are dry etched by oxygen plasma to release sacrificial photoresist. Sacrificial photoresist is released in acetone.

### 4.1.1. Sacrificial Photoresist Layer

In order to form a sacrificial layer for the microfluidic channel, a thick photoresist SPR220.7 determining the height of the microfluidic channel, is used. Otherwise, the channel may collapse. The patterning method for SPR220.7 is given in Appendix A. After that process, a sacrificial layer with a thickness of about 10 $\mu$m can be formed.

## 4.2. Microfluidic Channel Materials

Three different materials are utilized to fabricate microfluidic channel.

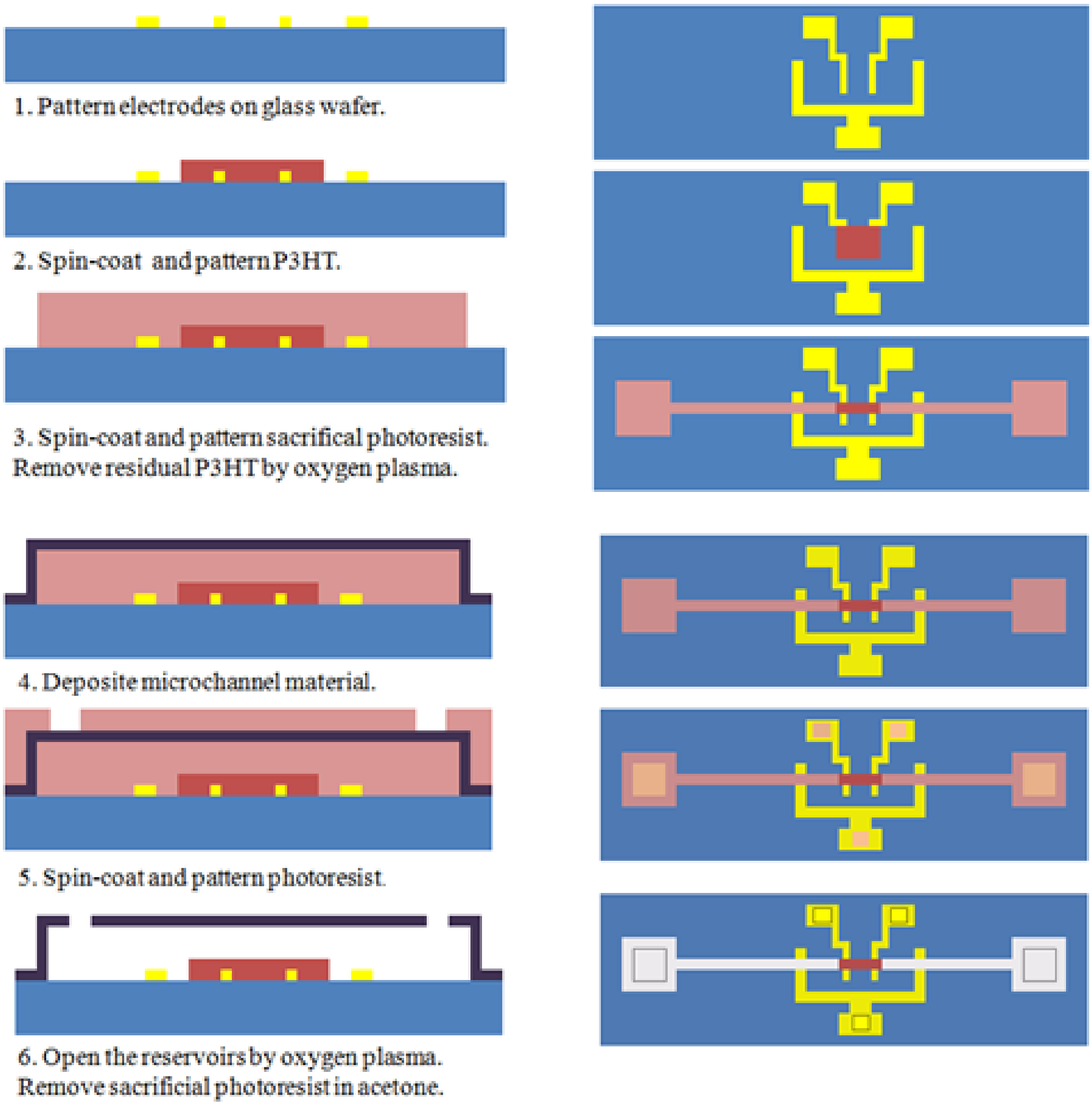


Figure 4.1. Parylene and PVA microfluidic channel integration process flow.

### 4.2.1. Polyvinyl Alcohol (PVA) Microfluidic Channel

Polyvinyl alcohol (PVA) is used as gate dielectric in OFETs [33]. It can be easily dissolved in water at room temperatures. But, after it is baked at high temperatures (about 140 $^{o}$C), it becomes insoluble due to crystallization of PVA [34]. It can be deposited from its solution by spin-coating providing the advantage of easy and cheap fabrication.

The primary work is to explore production of a PVA microfluidic channel before its OFET integration. Therefore, in order to get enough thick PVA film, aqueous solution of PVA in different concentrations is spin-coated over clean glass wafer. Since dilute solutions result in thin films, %25 PVA solution (60 g DI water and 20 g PVA) are used. To remove all bubbles in the solution, the solution is kept at 80 $^{o}$C for 3 hours. By means of this solution, PVA film thickness of about 10 $\mu$m is achieved. To remove completely the water in the film and harden it, it is firstly baked at 65 $^{o}$C for 1.5 hours and then at 140 $^{o}$C for 2 hours.

In order to see whether the microfluidic channel would collapse or not, sacrificial photoresist film is patterned on a glass wafer. Then, PVA solution is spin-coated at 2000 rpm. After the necessary steps are done as explained above, the reservoirs of the channel are opened using laser machining. Finally, the wafer is left in acetone for about 2 days to remove sacrificial photoresist. Figure 4.2 gives the photograph of microfluidic channels showing successful fluid flowing through the microfluidic channel. As a result, it is observed that adhesion of the PVA film to glass wafer is very good and the channel is opened successfully. An important point to pay attention is that during the baking at 140 $^{o}$C, water dissolved inside SPR220.07 can evaporate and disrupt the PVA film morphology. So, before spin-coating of PVA solution, SPR220.07 sacrificial layers should be baked at 140 $^{o}$C de for about 30 minutes.

After PVA microfluidic channels are fabricated successfully, the next step is to integrate the OFET to PVA microfluidic channels. For this purpose, the process flow in Figure 4.1 together with PVA film formation method is followed. Firstly, P3HT film is

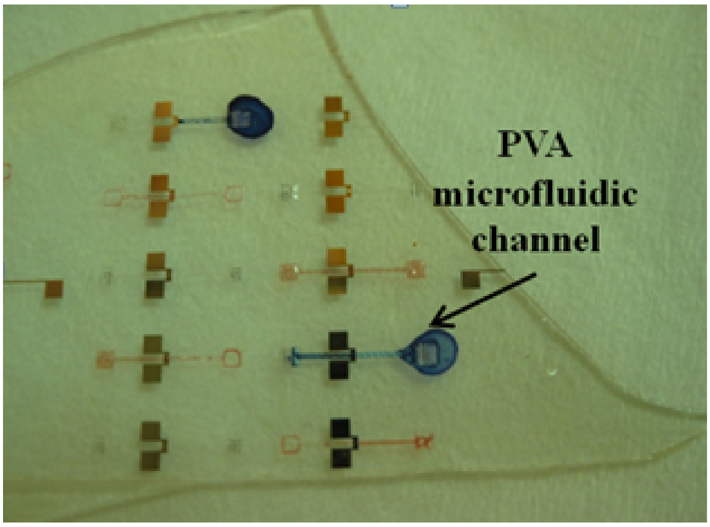


Figure 4.2. The photograph of PVA microfluidic channels showing the successful fluid flowing through the microfluidic channel.

patterned as seen in Figure 4.3. Then microfluidic channel over P3HT is formed. But, when the final devices are tested, it is seen that they do not work as a transistor. After searching for possible reasons, it is proven that baking both P3HT and photoresist at high temperatures to remove the water in PVA film leads to losses on the electrical characteristics of P3HT.

A possible solution to this can be to remove the photoresist layer before drying the PVA film. Thus, there would be no photoresist film over P3HT during baking. Figure 4.4 shows the microscope image of OFET integrated into PVA microfluidic channels. As seen, leaving the PVA film in acetone before completely drying it, results in collapsed and cracked microfluidic channels.

Therefore, although PVA microfluidic channels are independently produced and fluid flow through the channels are shown, OFET integration into this microfluidic channel cannot be realized due to process conditions.

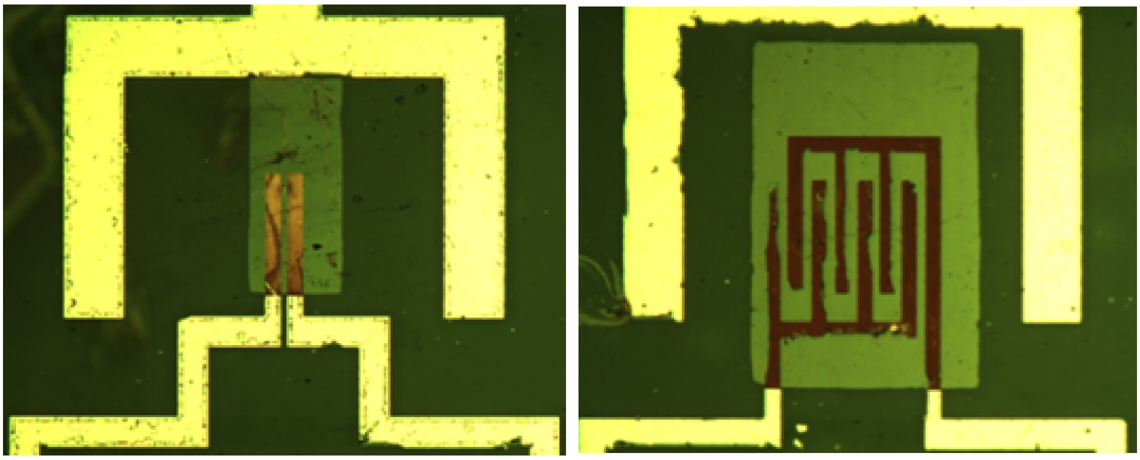

Figure 4.3. The microscope image of patterned P3HT before microfluidic channel integration.

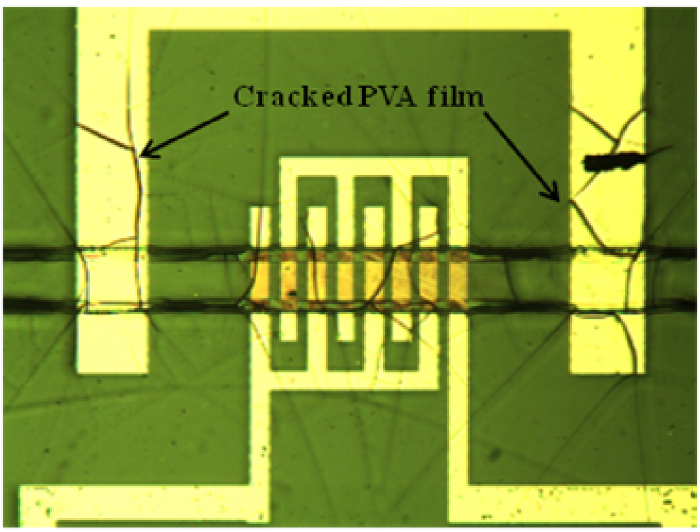


Figure 4.4. The microscope image of OFET integrated into PVA microfluidic channels.

### 4.2.2. Parylene Microfluidic Channel

Parylene is the general trade name of poly (p-xylylene) polymers. This material fabrication technology makes use of conformal and pin-hole free coating of the parylene film, being a good electrical insulator, chemically inert, biocompatible and deposited at room temperatures. On the other hand, it has the disadvantage of requiring an expensive machine increasing the cost of the fabrication. Also, another restriction is resulted from low adhesion to the glass surface. Therefore, adhesion promoter should be applied to the vacuum chamber walls before starting to deposition. There are three mostly used types of parylene, parylene-C, parylene-N and parylene-D. Especially, parylene-C is preferred since it is low toxic, a good barrier to moisture and durable to biological corrosion [35].

Normally, it is a dimer in powder form and it is transformed into a gaseous state (turning it into monomer) by heating. When it is introduced to a very low pressure vacuum chamber and cools, it is polymerized and can be deposited on most surfaces at room temperature.

To fabricate OFETs integrated into parylene microfluidic channel, again the process flow in Figure 4.1 is followed. Using 10 g of parylene-C, about 6 $\mu$m thick parylene film is deposited as microfluidic channel walls. The photograph of fabrication results can be shown in Figure 4.5. It shows the flow of colored fluid through the microfluidic channel. Also, DI water can easily enter the microfluidic channel. Figure 4.6 shows the microscope image of OFET integrated into parylene microfluidic channels.

$I_{DS}$-$V_{DS}$ characteristics of OFET integrated into parylene microfluidic channel can be seen Figure 4.7. $I_{OFF}$ and $I_{ON}$ are 0.15 nA and 0.65 nA, respectively, leading to on-off ratio of about 4. But, the currents decrease very much compared to values before patterning. Of course, the problem is greatly caused by microfabrication processes. On the other hand, vacuuming during the parylene deposition can be another factor to explain this decrease.

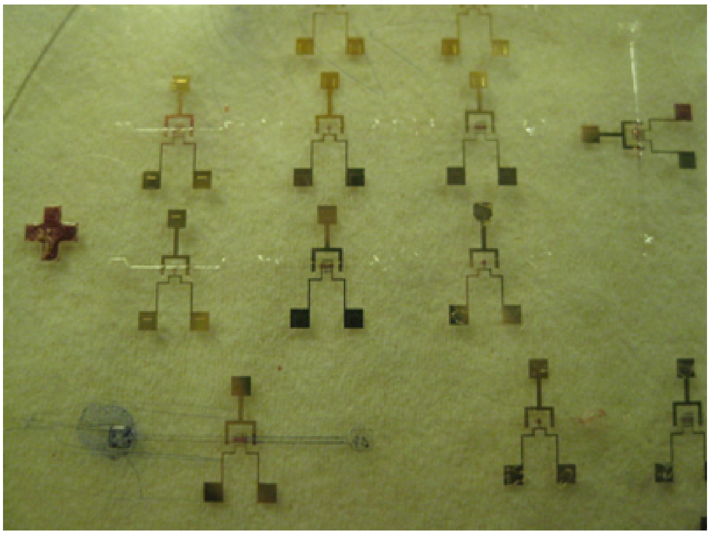

Figure 4.5. The photograph of parlyene microfluidic channels showing the successful fluid flowing through a microfluidic channel.

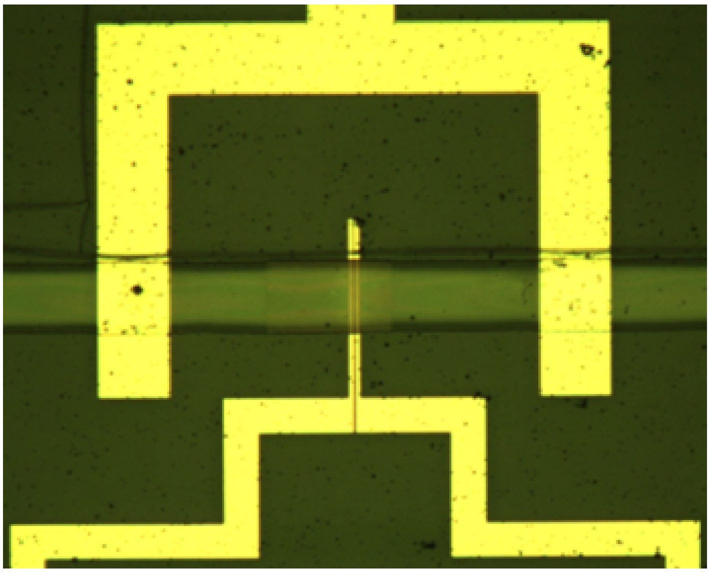

Figure 4.6. The microscope image of OFET integrated into parylene microfluidic channels.

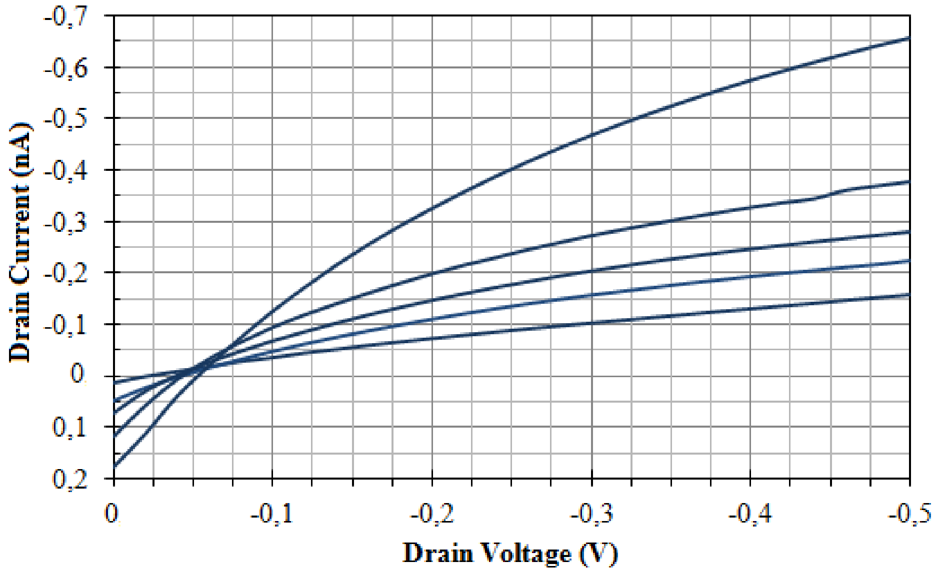


Figure 4.7. $I_{DS}$-$V_{DS}$ characteristics of OFET integrated into parylene microfluidic channel.

#### 4.2.3. Polydimethylsiloxane (PDMS) Microfluidic Channel

It is clear from microfluidic channel integration experiments with PVA and parylene that too many fabrication processes over P3HT affect negatively its electrical characteristics. In order to prevent P3HT from microfabrication processes, another material, PDMS, is explored. It depends on bulk micromachining instead of surface micromachining as given in Figure 4.8. It takes advantage of doing less fabrication processes since PDMS microfluidic channel is formed on another mold wafer. However, one shortcoming of PDMS microfluidic channels resides in the difficulties of alignment over the patterned organic semiconductor. Besides, since it is hydrophobic, it is hard to fill the microfluidic channel with DI water.

As seen from Figure 4.8, firstly, sacrificial photoresist is spin-coated and patterned on a wafer. Then 30 ml of the silicone elastomer and 3 ml of its curing agent are mixed giving the ratio of 10:1. After the mixture is stirred with a pipette until it becomes homogenous, it is poured over the mold. It is left for one day in ambient air and all bubbles in the film are removed. When PDMS becomes solid after a day, the reservoirs

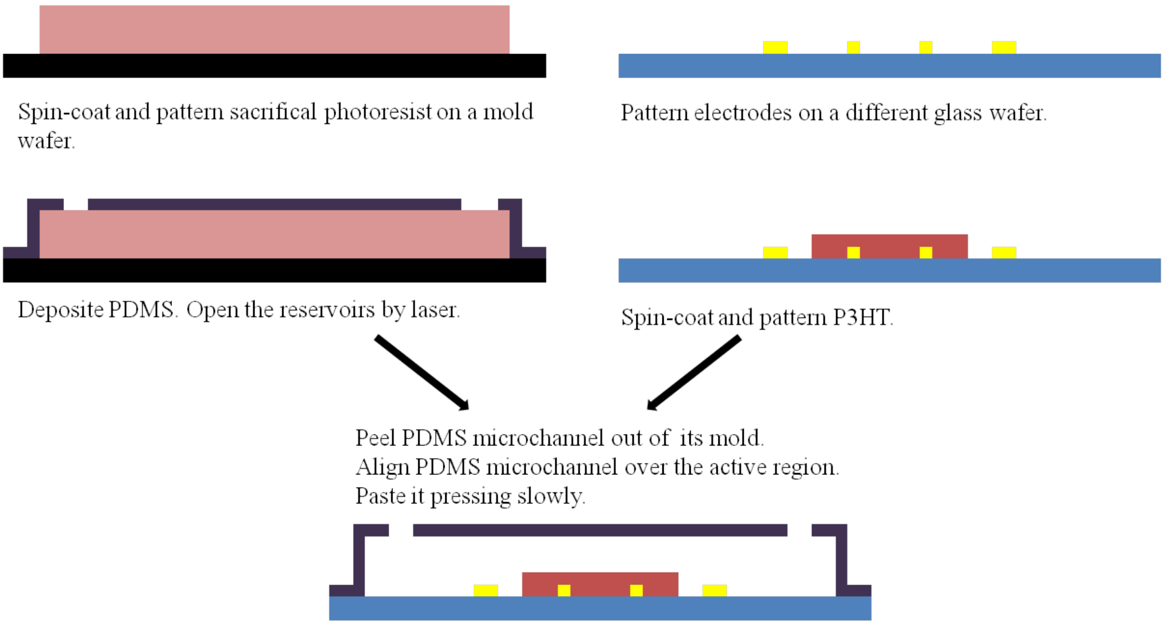


Figure 4.8. The microscope image of OFET integrated to PDMS microfluidic channel.

of the microfluidic channels can be opened with laser machining. Finally, they are peeled off the mold. Transistors are fabricated on another glass wafer. After electrodes are formed on the glass wafer, P3HT is patterned over source and drain electrodes as in PVA integration process. PDMS interface is activated with oxygen plasma for 5 minutes to be able to get a good bond between PDMS and glass. After oxygen plasma, PDMS microfluidic channels are immediately aligned over active region and pressed for a while. Oxygen plasma is also needed to render the PDMS surface hydrophilic since it is normally hydrophobic. Therefore, DI water can more easily enter the channel. Figure 4.9 shows the microscope image of OFET successfully integrated to PDMS microfluidic channel.

Figure 4.10 shows the photograph taken from test setup of OFET integrated to the PDMS microfluidic channel. DI water is dropped over the right reservoir. $I_{DS}$-$V_{DS}$ characteristics of OFET integrated to the PDMS microfluidic channel can be seen in Figure 4.11. $I_{OFF}$ and $I_{ON}$ are 2 nA and 21 nA, respectively, leading to on-off ratio of about 10. Normally, after patterning P3HT with photoresist, on current reduces to a few hundred nAs. Additionally, the microfluidic channel integration decreases the

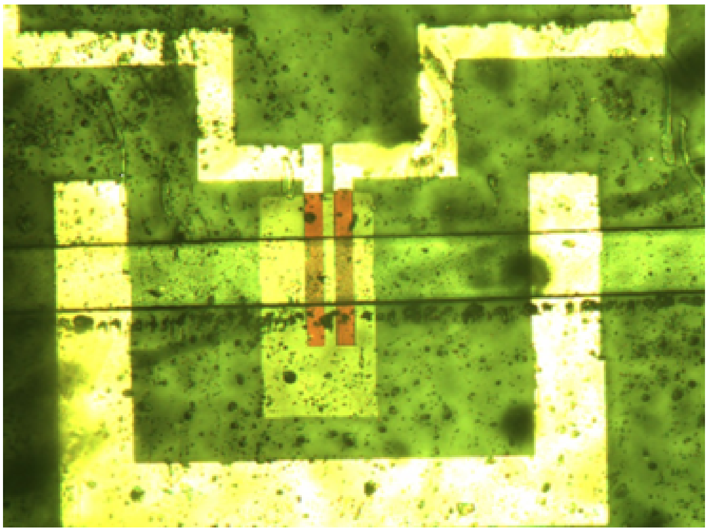

Figure 4.9. The microscope image of OFET integrated to PDMS microfluidic channel.

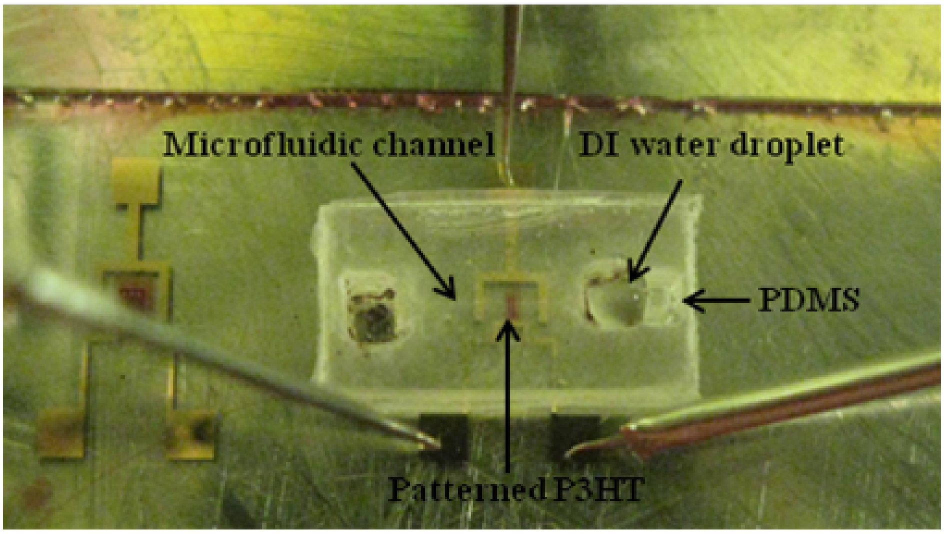


Figure 4.10. The photograph taken from test setup of OFET integrated to the PDMS microfluidic channel.

effective channel width to one third of the original value. Therefore, it seems reasonable to obtain $I_{ON}$ values smaller than 100 nA.

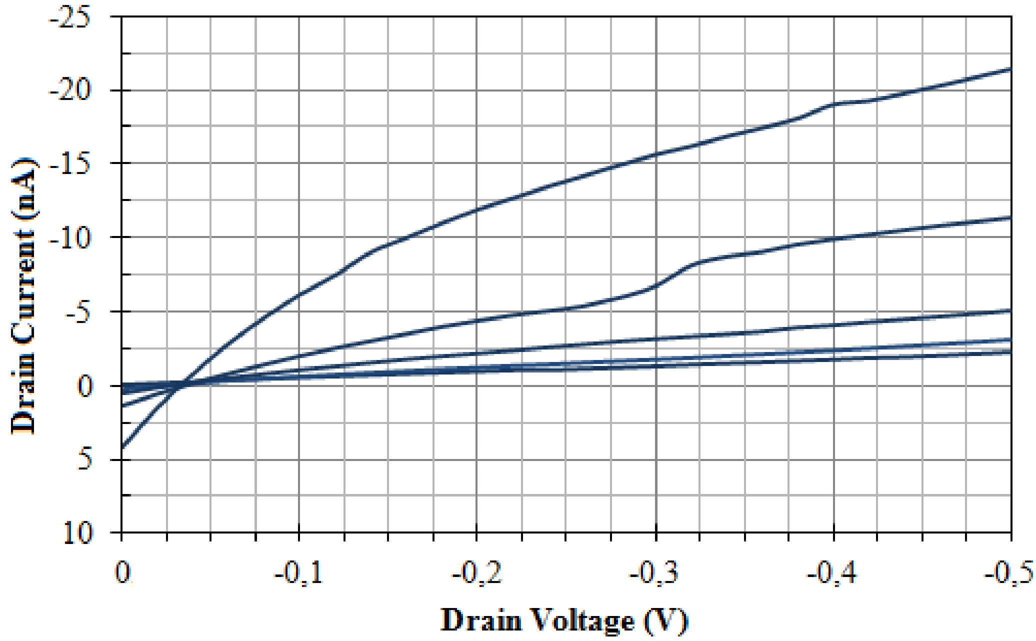


Figure 4.11. $I_{DS}$-$V_{DS}$ characteristics of OFET integrated into PDMS microfluidic channel.

# 5. CONCLUSION AND FUTURE WORK

The conclusions about the thesis can be summarized as follows

- Using DI water as gate insulator, polymer field effect transistors (polymer FETs) possessing current values of a few $\mu$As are succeeded while operation voltages of them are decreased below 1V.
- Planar OFET topology operating successfully as a field effect transistor providing on-off ratio of about 50 is designed and introduced. At the same time, they show clear saturation effect and square-law behavior.
- It is shown that for top-gate, bottom-contact topology, to deposite P3HT, spin-coating leads higher mobility values than drop-casting.
- P3HT film is successfully patterned by PR1828 and SPR220.07.
- PVA microfluidic channels providing liquid flow are successfully formed by using cheap and simple fabrication techniques.
- On-off ratios of 4 and 10 are obtained making use of planar polymer FETs integrated into parylene and PDMS microfluidic channel, respectively.

There are also remaining issues to be searched and improved. Firstly, P3HT patterning can be optimized so that high currents and on-off ratios with PDMS microfluidic channel integration can be obtained. Then, tubes, syringes and syringe pumps can be utilized to observe the sensor characteristics of hybrid structure. On the other hand, planar OFET integration into parylene microfluidic channel with deposition of P3HT by electropolymerization can be searched. In addition, P3HT can be functionalized to detect a special analyte.

# APPENDIX A: SPR220.07 PROCESS FLOW

To pattern SPR220.07, the below process flow is followed in the experiments.

- A clean wafer is prebaked at 120 $^oC$ for 5 minutes using a hotplate.
- The wafer is spin-coated with SPR220.07 for 30 seconds at 2000 rpm.
- Firstly, the wafer is softbaked above 1mm over the hot plate at 105 $^oC$ for 60 seconds and then it is directly left over hot plate at 105 $^oC$ for 90 seconds.
- It is exposed to UV light for 165 seconds at 490 Watts.
- Rehydration step for 45 minutes is allowed.
- A post exposure bake is performed at 105 $^oC$ for 90 seconds.
- It is developed in MF24A for 2 minutes.
- Finally, it is immediately rinsed in DI water and dried with nitrogen.

# APPENDIX B: PR1828 PROCESS FLOW

To pattern PR1828, the below process flow is followed in the experiments.

- A clean wafer is prebaked at 120 $^{o}$C for 5 minutes using a hotplate.
- The wafer is spin-coated with PR1828 for 30 seconds at 2000 rpm.
- The wafer is softbaked at 90 $^{o}$C for 60 seconds.
- It is exposed to UV light for 60 seconds at 490 Watts.
- It is developed in MF24A for 1 minutes.
- Finally, it is immediately rinsed in DI water and dried with nitrogen.

# REFERENCES

1. Kergoat, L., B. Piro, M. Berggren, G. Horowitz and M.-C. Pham, "Advances in organic transistor-based biosensors: from organic electrochemical transistors to electrolyte-gated organic field-effect transistors", *Analytical and Bioanalytical Chemistry*, Vol. 402, pp. 1813–1826, 2012.

2. Sirringhaus, H., "Device Physics of Solution-Processed Organic Field-Effect Transistors", *Advanced Materials*, Vol. 17, No. 20, pp. 2411–2425, 2005.

3. Hasegawa, T. and J. Takeya, "Organic field-effect transistors using single crystals", *Science and Technology of Advanced Materials*, Vol. 10, No. 2, p. 024314, 2009.

4. Bartic, C. and G. Borghs, "Organic thin-film transistors as transducers for (bio) analytical applications", *Analytical and Bioanalytical Chemistry*, Vol. 384, pp. 354–365, 2006.

5. Panzer, M. J. and C. D. Frisbie, "Exploiting Ionic Coupling in Electronic Devices: Electrolyte-Gated Organic Field-Effect Transistors", *Advanced Materials*, Vol. 20, No. 16, pp. 3177–3180, 2008.

6. Ono, S., K. Miwa, S. Seki and J. Takeya, "High-performance organic field-effect transistors with binary ionic liquids", *Organic Electronics*, Vol. 10, No. 8, pp. 1579–1582, 2009.

7. Lee, J., M. J. Panzer, Y. He, T. P. Lodge and C. D. Frisbie, "Ion Gel Gated Polymer Thin-Film Transistors", *Journal of the American Chemical Society*, Vol. 129, No. 15, pp. 4532–4533, 2007.

8. Shim, J., C. H. Lui, T. Y. Ko, Y.-J. Yu, P. Kim, T. F. Heinz and S. Ryu, "Water-Gated Charge Doping of Graphene Induced by Mica Substrates", *Nano Letters*, Vol. 12, No. 2, pp. 648–654, 2012.

9. Braga, D. and G. Horowitz, "High-Performance Organic Field-Effect Transistors", *Advanced Materials*, Vol. 21, No. 14-15, pp. 1473–1486, 2009.

10. Kergoat, L., L. Herlogsson, D. Braga, B. Piro, M.-C. Pham, X. Crispin, M. Berggren and G. Horowitz, "A Water-Gate Organic Field-Effect Transistor", *Advanced Materials*, Vol. 22, No. 23, pp. 2565–2569, 2010.

11. Tanase, C., P. W. Blom, E. J. Meijer and D. M. d. Leeuw, "Charge transport in disordered organic field-effect transistors", *MRS Proceedings*, Vol. 725.

12. Horowitz, G., "Organic Field-Effect Transistors", *Advanced Materials*, Vol. 10, No. 5, pp. 365–377, 1998.

13. Afzali, A., C. D. Dimitrakopoulos and T. L. Breen, "High-Performance, Solution-Processed Organic Thin Film Transistors from a Novel Pentacene Precursor", *Journal of the American Chemical Society*, Vol. 124, No. 30, pp. 8812–8813, 2002.

14. Majewski, L. A., J. W. Kingsley, C. Balocco and A. M. Song, "Influence of processing conditions on the stability of poly(3-hexylthiophene)-based field-effect transistors", *Applied Physics Letters*, Vol. 88, No. 22, pp. 222108 –222108–3, 2006.

15. Chang, J.-F., B. Sun, D. W. Breiby, M. M. Nielsen, T. I. Sölling, M. Giles, I. McCulloch and H. Sirringhaus, "Enhanced Mobility of Poly(3-hexylthiophene) Transistors by Spin-Coating from High-Boiling-Point Solvents", *Chemistry of Materials*, Vol. 16, No. 23, pp. 4772–4776, 2004.

16. Zen, A., J. Pflaum, S. Hirschmann, W. Zhuang, F. Jaiser, U. Asawapirom, J. Rabe, U. Scherf and D. Neher, "Effect of Molecular Weight and Annealing of Poly(3-hexylthiophene)s on the Performance of Organic Field-Effect Transistors", *Advanced Functional Materials*, Vol. 14, No. 8, pp. 757–764, 2004.

17. Kline, R., M. McGehee, E. Kadnikova, J. Liu and J. Frechet, "Controlling the Field-Effect Mobility of Regioregular Polythiophene by Changing the Molecular

Weight", *Advanced Materials*, Vol. 15, No. 18, pp. 1519–1522, 2003.

18. Anthony, J. E., A. Facchetti, M. Heeney, S. R. Marder and X. Zhan, "n-Type Organic Semiconductors in Organic Electronics", *Advanced Materials*, Vol. 22, No. 34, pp. 3876–3892, 2010.

19. Chua, L.-L., J. Zaumseil, J.-F. Chang, E. C.-W. Ou, P. K.-H. Ho, H. Sirringhaus and R. H. Friend, "General observation of n-type field-effect behaviour in organic semiconductors", *Nature*, Vol. 434, pp. 194–199, 2005.

20. Herlogsson, L., *Electrolyte-Gated Organic Thin-Film Transistors*, Ph.D. Thesis, Linkoping Studies in Science and Technology, 2011.

21. Wang, G., J. Swensen, D. Moses and A. J. Heeger, "Increased mobility from regioregular poly(3-hexylthiophene) field-effect transistors", *Journal of Applied Physics*, Vol. 93, No. 10, pp. 6137 –6141, 2003.

22. Bartic, C., H. Jansen, A. Campitelli and S. Borghs, "Ta2O5 as gate dielectric material for low-voltage organic thin-film transistors", *Organic Electronics*, Vol. 3, No. 2, pp. 65 – 72, 2002.

23. Wang, G., D. Moses, A. J. Heeger, H.-M. Zhang, M. Narasimhan and R. E. Demaray, "Poly(3-hexylthiophene) field-effect transistors with high dielectric constant gate insulator", *Journal of Applied Physics*, Vol. 95, No. 1, pp. 316 –322, 2004.

24. Yoon, M.-H., H. Yan, A. Facchetti and T. J. Marks, "Low-Voltage Organic Field-Effect Transistors and Inverters Enabled by Ultrathin Cross-Linked Polymers as Gate Dielectrics", *Journal of the American Chemical Society*, Vol. 127, No. 29, pp. 10388–10395, 2005.

25. Jang, Y., D. H. Kim, Y. D. Park, J. H. Cho, M. Hwang and K. Cho, "Low-voltage and high-field-effect mobility organic transistors with a polymer insulator", *Applied Physics Letters*, Vol. 88, No. 7, pp. 072101 –072101–3, 2006.

26. Panzer, M. J. and C. D. Frisbie, "Polymer Electrolyte-Gated Organic Field-Effect Transistors: Low-Voltage, High-Current Switches for Organic Electronics and Testbeds for Probing Electrical Transport at High Charge Carrier Density", *Journal of the American Chemical Society*, Vol. 129, No. 20, pp. 6599–6607, 2007.

27. Ono, S., K. Miwa, S. Seki and J. Takeya, "A comparative study of organic single-crystal transistors gated with various ionic-liquid electrolytes", *Applied Physics Letters*, Vol. 94, No. 6, pp. 063301 –063301–3, 2009.

28. Bard, A. J. and L. R. Faulkner, *Electrochemical Methods: Fundamentals and Applications*, John Wiley & Sons, Inc., New York, NY, USA, 2000.

29. Panzer, M. J., C. R. Newman and C. D. Frisbie, "Low-voltage operation of a pentacene field-effect transistor with a polymer electrolyte gate dielectric", *Applied Physics Letters*, Vol. 86, No. 10, pp. 103503 –103503–3, 2005.

30. Mabeck, J. T., J. A. DeFranco, D. A. Bernards, G. G. Malliaras, S. Hocdé and C. J. Chase, "Microfluidic gating of an organic electrochemical transistor", *Applied Physics Letters*, Vol. 87, No. 1, p. 013503, 2005.

31. Balocco, C., L. Majewski and A. Song, "Non-destructive patterning of conducting-polymer devices using subtractive photolithography", *Organic Electronics*, Vol. 7, No. 6, pp. 500 – 507, 2006.

32. Majewski, L. A. and A. M. Song, "Extended storage time of poly(3-hexylthiophene) field-effect transistors via immersion in common solvents", *Journal of Applied Physics*, Vol. 102, No. 7, p. 074515, 2007.

33. Singh, T., F. Meghdadi, S. Günes, N. Marjanovic, G. Horowitz, P. Lang, S. Bauer and N. Sariciftci, "High-Performance Ambipolar Pentacene Organic Field-Effect Transistors on Poly(vinyl alcohol) Organic Gate Dielectric", *Advanced Materials*, Vol. 17, No. 19, pp. 2315–2320, 2005.

34. Zhang, Q. and V. Subramanian, "Label-free low-cost disposable DNA hybridization detection systems using organic TFTs", *Electron Devices Meeting, 2007. IEDM 2007. IEEE International*, pp. 229 –232, 2007.

35. Man, P., D. Jones and C. Mastrangelo, "Microfluidic plastic capillaries on silicon substrates: a new inexpensive technology for bioanalysis chips", *Micro Electro Mechanical Systems, 1997. MEMS '97, Proceedings, IEEE., Tenth Annual International Workshop on*, pp. 311 –316, 1997.